HLA-E-restricted SARS-CoV-2-specific T cells from convalescent COVID-19 patients suppress virus replication despite HLA class Ia down-regulation

Title:

HLA-E Restricted SARS-CoV-2 Specific T Cells from Convalescent COVID19 Patients Suppress Virus Replication Despite HLA Class Ia Downregulation

Authors: Hongbing Yang[1, 2+ *], Hong Sun[1,2,3+], Simon Brackenridge[1], Xiaodong Zhuang[4], Peter A C Wing[2, 4], Max Quastel[1], Lucy Walters[1], Lee Garner[1], Beibei Wang[2,5], Xuan Yao[2,5], Suet Ling Felce[2], Yanchun Peng[5], Shona Moore[6], Bas W.A. Peeters[1], Margarida Rei[7], Joao Canto Gomes[8, 9], Ana Tomas[10, 11], Andrew Davidson[12] , Malcolm G. Semple[6,16], Lance C.W. Turtle[6.13], Peter J.M. Openshaw[14], J. Kenneth Baillie[15], Alexander J. Mentzer[16], Paul Klenerman[17], ISARIC-4C Investigators[18], Persephone Borrow[1], Tao Dong[2,5], Jane A McKeating[2,4*], Geraldine M Gillespie[1*], Andrew J McMichael[1*]

Affiliations:

1. Centre for Immuno-Oncology, Nuffield Dept of Clinical Medicine, University of Oxford, Old Road Campus, Oxford
2. Chinese Academy of Medical Sciences Oxford Institute, Old Road Campus, Oxford
3. Key Laboratory of AIDS Immunology, Department of Laboratory Medicine, First Affiliated Hospital of China Medical University, Shenyang, China
4. Nuffield Dept of Clinical Medicine, NDM Research Building, University of Oxford, Old Road Campus, Oxford
5. MRC Human Immunology Unit, MRC Weatherall Institute of Molecular Medicine, Oxford University
6. Health Protection Research Unit in Emerging and Zoonotic Infections, Institute of Infection, Veterinary and Ecological Sciences, University of Liverpool
7. Ludwig Institute for Cancer Research, Old Road Campus, University of Oxford
8. Life and Health Sciences Research Institute, School of Medicine, University of Minho, Braga, Portugal
9. ICVS/3B's, PT Government Associate Laboratory, Braga, Portugal
10. Unidada de Investigacao em Patobiologia Molecular, Instituto Portugues de Oncologia de Lisboa Francisico Gentil E.P.E., Lisbon, Portugal
11. Chronic Diseases Research Centre, NOVA Medical School, Universidade NOVA de Lisboa, Lisbon, Portugal
12. School of Cellular and Molecular Medicine, University of Bristol, UK
13. Tropical & Infectious Disease Unit, Liverpool University Hospitals NHS Foundation Trust (member of Liverpool Health Partners)
14. National Heart and Lung Institute, Imperial College London, London
15. Roslin Institute, University of Edinburgh, Edinburgh,
16. Welcome Centre for Human Genetics, University of Oxford, Old Road Campus, Oxford
17. Peter Medawar Building for Pathogen Research and Translational Gastroenterology Unit, University of Oxford
18. International Severe Acute Respiratory Infection Consortium- Coronavirus Clinical Characterisation Consortium. https://isaric4c.net/about/authors/

+ Co-first authors

*Corresponding authors:

Email: Andrew J McMichael, andrew.mcmichael@ndm.ox.ac.uk; Geraldine M Gillespie, geraldine.gillespie@ndm.ox.ac.uk; Jane A McKeating, jane.mckeating@ndm.ox.ac.uk; Hongbing Yang, hongbing.yang@ndm.ox.ac.uk

Abstract:

Pathogen specific CD8+ T cell responses restricted by the non-polymorphic non-classical class Ib molecule HLA-E are rarely reported in viral infections. The natural HLA-E ligand is a signal peptide derived from classical class Ia HLA molecules that interacts with the NKG2/CD94 receptors to regulate natural killer (NK) cell functions – but pathogen-derived peptides can also be presented by HLA-E. Here we describe five peptides from severe acute respiratory syndrome coronavirus 2 (SARS-CoV-2) that elicited HLA-E restricted CD8+ T cell responses in COVID-19 convalescent patients. These T cell responses were present in the blood at frequencies similar to those reported for classical HLA-Ia-restricted anti-SARS-CoV-2 CD8+ T cells. HLA-E-peptide specific CD8+ T cell clones, which expressed diverse T cell receptors, suppressed SARS-CoV-2 replication in Calu-3 human lung epithelial cells. SARS-CoV-2 infection markedly downregulated classical HLA class I expression in Calu-3 cells and primary reconstituted human airway epithelia cells whereas HLA-E expression was not affected, enabling T cell recognition. Thus HLA-E restricted T cells could as important as classical T cells in controlling SARS-CoV-2 infection.

One Sentence Summary:

SARS-CoV-2 specific HLA-E restricted CD8+ T cells that are able to suppress virus replication *in vitro* despite classical HLA class Ia down-regulation are present in COVID-19 convalescent patients.

Main Text:

INTRODUCTION

Unlike the genetically polymorphic classical human leukocyte antigen (HLA)-A ,B and C molecules, just two major HLA-E allomorphs dominate at the population level, differing at a single amino acid at position 107 outside the peptide binding groove [1]. HLA-E is expressed on the surface of most cells at 1-5% of the level of the classical HLA-A and B molecules but is more abundant intracellularly [2-4]. There is some variation in expression in different tissues, with higher levels in lymphoid, renal and lung tissues (https://www.proteinatlas.org/ENSG00000204592-HLA-E/tissue). The primary role of HLA-E is to present a well conserved nonamer peptide, typically VMAPRTLVL (VL9), derived from the signal sequence of classical major histocompatibility complex class-Ia (MHC-Ia) molecules to the natural killer (NK) cell receptors CD94-NKG2A and CD94-NKG2C [5]. The former binds with higher affinity and delivers a dominant inhibitory signal to NK cells and to a subset of CD8+ T cells, that regulates their activity. Conservation of the signal peptide sequence and of the MHC-E peptide binding groove structure between mammalian species implies a common evolutionary origin for this important immune function. The signal peptide dominates the HLA-E bound peptidome, in contrast to the diverse peptide repertoire bound to the polymorphic classical HLA class Ia molecules [6].

MHC-E can also present pathogen derived peptides and altered self-peptides to CD8+ T cells, like classical MHC- Ia molecules [7-10]. However, the majority of reported antigenic peptide epitopes bind HLA-E with markedly lower affinity than the VL9 signal peptide [11,12] and consequently are likely to be out-competed by VL9 for binding to HLA-E in the endoplasmic reticulum (ER). This may help to explain why relatively few HLA-E restricted T cell responses have been described to date. However, if generation of, or access to, the VL9 signal peptide is

impaired or bypassed, other peptides can gain access to HLA-E and stimulate CD8+ T cell responses. Strong MHC-E restricted T cell responses have been reported in a few specific settings. One example is in rhesus monkeys following vaccination with Simian Immunodeficiency Virus (SIV) immunogens delivered by a particular strain of rhesus monkey cytomegalovirus (RhCMV68-1) [7]. This CMV vector has gene deletions [13] that alter viral tropism, while retaining genes that interfere with key elements of the classical antigen processing pathway that regulate trafficking of the host cell's VL9 signal peptide to MHC-E. Instead, a viral-derived VL9 peptide binds to MHC-E in the ER enabling traffic to the cell surface, where the complex is subsequently internalised and most likely gains access to other peptides within endosomes [14]. These infected cells can then prime CD8+ T cells [13,14] that are uniquely able to quench a challenge infection with SIV [7,14]. A second example is in human mycobacterial infections where antigen processing and HLA-E peptide binding occur in the phagolysosomes of infected macrophages rather than in the ER [15]. Most adult humans have readily detectable HLA-E restricted mycobacteria specific T cells in their blood [9].

In this study we assessed the role of HLA-E restricted T cells in the complex immune response to SARS-CoV-2. We tested the hypothesis that SARS-COV-2 inhibition of classical HLA-I expression allows HLA-E restricted CD8+ T cell responses to suppress virus replication. We found that there were readily detectable, previously unrecognized, CD8+ T cell responses to viral peptides presented by HLA-E in convalescent patients. Furthermore, these T cells were able to suppress virus replication in an experimentally infected human lung epithelial cell line. SARS-CoV-2 down-regulated surface expression of classical HLA class Ia molecules while having a minimal effect on the expression of HLA-E.

RESULTS

Identification of SARS-CoV-2-derived HLA-E binding peptides

Twenty-nine nonamer SARS-CoV-2 peptides derived from all open reading frames annotated in the reference genome (NC_045512.2) that were predicted to bind HLA-E by NetMHC4.0 [16] or by an in-house binding data informed algorithm [11] (Table S1) were selected for evaluation. Peptides P001–P010 represent the top HLA-E binders predicted by NetMHC4.0 [16]. Peptides P011–P029 were selected from 216 predicted peptides that possessed the HLA-E peptide binding motif previously reported [12]. This requires hydrophobic primary anchor residues at position 2 [M, I, L, V, A, F or Q] and position 9 [L, F, I, V or M], plus the presence of a proline between positions 3 and 7 of the peptide. All peptides were tested for binding to HLA-E by a UV peptide-exchange enzyme-linked immunosorbent assay (ELISA) [11] and single chain peptide-β2m-HLA-E trimer (SCT) cell surface expression method [7]. Peptide binding data generated by these two independent assays showed strong correlation (R^2=0.713, p<0.0001 *Prism Pearson correlation analysis*) (Fig. 1A-B) for peptides with the strongest binding signals – which included four predicted by NetMHC4.0 and two from our modified algorithm [11,12]. The five strongest binding peptides, which came from Spike and ORF1ab proteins, were highly conserved across all SARS-CoV-2 strains, as shown in Fig. S1.

The five highest binding SARS CoV-2 peptides were further validated by differential scanning fluorimetry (DSF) to assess the thermal stability of HLA-E bound to these peptides [12]. These data indicated that peptide 001, VMPLSAPTL [17], bound to HLA-E almost as well as VL9, so that stable conventional refolded tetramers could be made, whereas the other peptides bound in the range where they required stabilization by maintenance in a molar excess of peptide [18]. This was achieved by using the UV exchange method to introduce individual peptides into HLA-E initially refolded with an UV sensitive version of the VL9 peptide, and then

maintaining these samples in molar excess peptide following tetramerization and throughout storage[11,19]. In this way we were able to generate five stable HLA-E-peptide tetramers that bound T cell receptors with sufficient avidity to enable detection by flow cytometry[12].

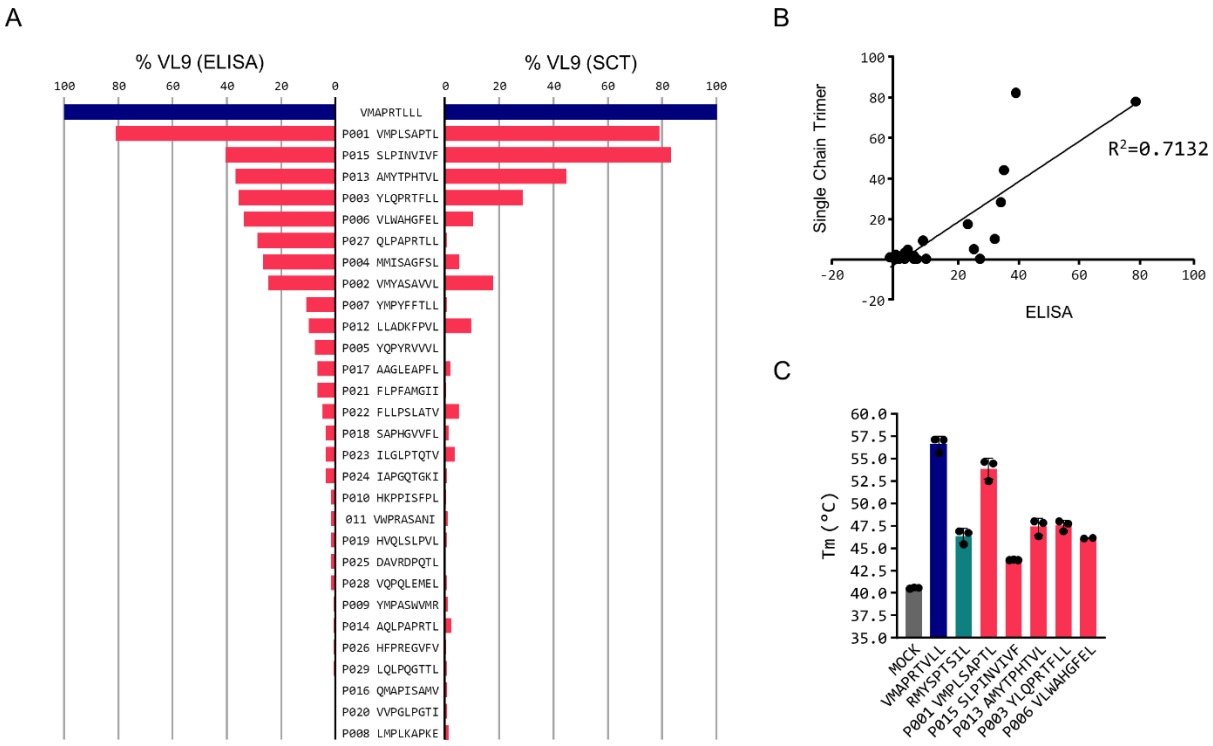

Fig. 1. Identification of HLA-E binding peptides using multiple strategies

A, NetMHC and in-house algorithm predicted SARS-CoV-2 derived-peptides were screened using both a UV peptide-exchange HLA-E binding ELISA assay and a single-chain trimer (SCT) HLA-E cell-surface expression assay. For ELISA assay-derived binding data, the percentage of absorbance signals for individual peptides were normalized to the VL9 positive control signals (%VL9) to rank HLA-E binding strength. For the SCT assay, the mean intensity for each tested peptide was normalized to that of the VL9 (%VL9) control. Tested peptide, red; VL9, positive control, dark blue. For ELISA-based screens, three independent peptide exchange reactions were performed per individual peptide (n=3), with 2 technical replicas per peptide tested in ELISA screens. The SCT assay was performed in triplicate. **B**, Prism Pearson correlation analysis of SCT and ELISA assays showed strong correlation (R^2=0.713, p<0.0001). **C**, The thermal melt temperature (Tm) of peptide-free HLA-E-β2m complexes pulsed with 100M excess of the top 5 ELISA-ranked SARS-CoV-2 peptide binders was determined by differential scanning fluorimetry (DSF). The positive control VL9 peptide and the previously reported HLA-E binding peptide, RL9HIV, were included for reference. SARS-CoV-2 peptide HLA-E, red; HIV Gag RL9, green; VL9, blue; mock, grey.

HLA-E restricted SARS-CoV-2-specific CD8+ T cells in convalescent COVID-19 patients

We employed five HLA-E SARS-CoV-2 peptide tetramers (P001, P003, P006, P013 and P015) to investigate whether SARS-CoV-2 specific CD8 cells could be detected in convalescent COVID-19 patients. Tetramer positive cells were gated on live $CD3^{+}CD4^{-}CD8^{+}$ singlets which were $CD56^{-}$ and $CD94^{-}$ to exclude NKG2/CD94 receptor expressing cells (Fig. S2A). We excluded NKG2 receptor binding by generating NKG2A and NKG2C tetramers that they failed to bind to SARS-CoV-2 peptide-HLA|-E expressed on transfected 293T cells, in contrast to the VL9-HLA-E control (Fig. S2B).

Peripheral blood mononuclear cells (PBMCs) from 9 healthy donors collected in 2019 prior to the COVID-19 pandemic were stained with these HLA-E tetramers to establish the level of background staining from naïve donors. The mean + 2 standard deviations (SD) gave a threshold for positive staining of >0.09% of CD8+ T cells (Fig. S3A).

In an initial study, we stained PBMCs from 5 COVID-19 convalescent patients, 3 sampled after mild infection (presenting to hospital early in the pandemic but never requiring oxygen) and 2 after recovering from severe disease, requiring supplemental oxygen but not assisted ventilation. Since HLA-E and HLA-A2 share an overlapping peptide binding motif [20] we selected HLA-A2 negative patients to avoid HLA-A2 presentation of the peptides. We identified SARS-CoV-2-specific CD8+ T cells for 3 different peptides (P001, P006 and P015), with observed differences between patients in terms of the magnitudes (0.1-0.6% of CD8+ T cells) and breadth of responses (Fig. S3B).

In order to further confirm the population detected by tetramer was truly peptide specific, paired HLA-E tetramers conjugated with Allophycocyanin (APC) or Phycoerythrin (PE) were used to stain PBMC from 5 convalescent patients who had a large number of PBMC stored. We also included an HLA-E tetramer refolded with an HLA-E binding *Mycobacterium tuberculosis* peptide Mtb44 (RLPAKAPLL) as a negative tetramer control to test the

background staining for each patient. A minimum of 1 million live PBMC was used per stain and >250,000 live CD8+ T cells were acquired (Fig 2A). The control HLA-E-Mtb44 tetramer showed low background staining with a mean of double tetramer positive cells at 0.05% of CD8+ T cells (range 0.01% to 0.080%). SARS-CoV2 peptide specific population identified as double tetramer positive were detected in all 5 patients with breadth of 1 to 3 peptides being recognised and magnitude of 0.16% to 0.56% of CD8+ T cells after subtracting background staining of HLA-E-Mtb44 tetramer (Fig 2B).

The detection of HLA-E restricted CD8 responses at levels comparable to those of conventional HLA Ia-restricted T cells in PBMC of convalescent patients [21-26] led us to study a larger group of 22 convalescent patients, recruited in Liverpool on the ISARIC4C clinical characterisation protocol (CCP01118-02366 in Table S2). These patients were stratified into those recovering from mild (n=8) or more severe disease (n=14), where the latter group experienced intensive treatment unit (ITU) admission and/or required oxygen before disease resolution. Patients from both cohorts did not differ in age or time post symptoms when considering severity categories (Fig. S4A-C). HLA-E tetramer positive CD8+ T cells were detected in PBMCs from 18 patients, with a mean frequency of 0.22% CD8+ T cells (IQR, 0.10%-0.39%). These frequencies are comparable to those of classical HLA Class Ia restricted SARS-CoV-2 specific T cells reported previously [21-26]. We noted that the frequencies of tetramer positive CD8+ T cells were significantly lower in patients who recovered from mild infections, 0.11% (IQR, 0.00%-0.23%), compared with severe convalescent patients, 0.30% (IQR, 0.12%-0.52%) (p= 0.03, Mann Whitney U test, Fig. 2C). In addition, the number of tetramers that gave detectable staining of CD8+ T cells was greater in the severe disease group. Peptide P001 staining, which was detected in 14 patients, was the most common epitope recognised, but the frequency of P001-tetramer binding cells by itself did not accurately reflect

239 the total response (Fig. 2C). These findings suggest that higher levels of virus exposure in
240 severe patients [27,28] elicited HLA-E restricted T cell responses that were of higher magnitude
241 and broader, at least in those that recovered from their infection, than those in patients with
242 mild disease.
243
244 In order to explore the antiviral functions of HLA-E restricted SARS-CoV-2 specific T cells,
245 we generated SARS-CoV-2 specific HLA-E restricted CD8+ T cell clones. CD8 positive
246 PBMCs from two convalescent patients, Pt1016 (mild disease) and Pt1504 (severe disease),
247 were stained with a mixture of three HLA-E tetramers (peptides P001, P006 and P015).
248 Tetramer positive CD8+ T cells were sorted and seeded at <0.4 cells per well in microtiter trays
249 and cultured with irradiated allogeneic feeder cells, phytohemagglutinin (PHA) and
250 interleukin-2 (IL-2). 87 clones proliferated and HLA-E tetramer staining revealed 9 positive
251 clones from Pt1016 and 4 positive clones from Pt1504 (Fig. 2D). When co-stained with single
252 peptide HLA-E tetramers labelled with different fluorophores, each clone demonstrated single
253 peptide specificity (Fig. 2E, 2F). 8 of 13 clones were specific for peptide P015, whereas 3
254 clones were peptide P001-specific, and 2 clones were specific for peptide P006 (Fig. 2F).
255 These findings ruled out non-specific binding to HLA-E through their TCRs or other receptors.
256
257 The T cell receptors (TCRs) of the clones were sequenced using the SMART (Switching
258 Mechanism at 5'end of RNA Template) [29] and 5'RACE (5'Rapid Amplification of cDNA Ends)
259 techniques [30]. Each expressed a single TCR β chain, with a single α chain in 10. 3 out of 13
260 clones expressed two α chains (Table 1). No shared TCRs were found amongst these clones,
261 but two of three P001 specific T cell clones used TRAV21 and three out of eight P015 specific
262 clones utilized TRBJ2-1.
263

The frequency of tetramer positive cells within the 13 clones ranged from 0.7%-43% of CD8+T cells (Fig. 2D). We arbitrarily considered with <5% staining not to be SARS-CoV-2 specific; although they were clonal populations, they may have had other primary specificities with weak additional cross reactivity to peptide-HLA-E complexes. Those with higher binding were highly likely to be peptide-HLA-E specific. Incomplete tetramer staining has been previously reported for HLA-E-restricted HIV-1 specific CD8+ T cell clones [31] and also for T cells detected with MHC Class Ia-peptide tetramers [32,33]. Stable binding by tetramers depends on the avidity conferred by binding of two or more of the HLA-E-peptide complexes within the tetramer to TCRs on T cells. If overall TCR density is low, T cells at the lower end of the Gaussian distribution would bind only one of the four HLA-E-peptide components of the tetramer, so that binding would be dependent only on affinity, which is low for TCRs [34-36]. T cells with higher TCR density could bind two or more peptide-HLA complexes within the tetramer, gaining avidity; for antibodies this can increase binding >100-fold [37]. If tetramer only stained T cells when two or more HLA-E-peptide subunits bound, this would give bimodal, all or none, binding as observed. When we omitted the wash step after initial tetramer binding[38] before addition of anti-CD8 antibodies, higher levels of specific staining were observed but with higher backgrounds (Fig. S2C, D).

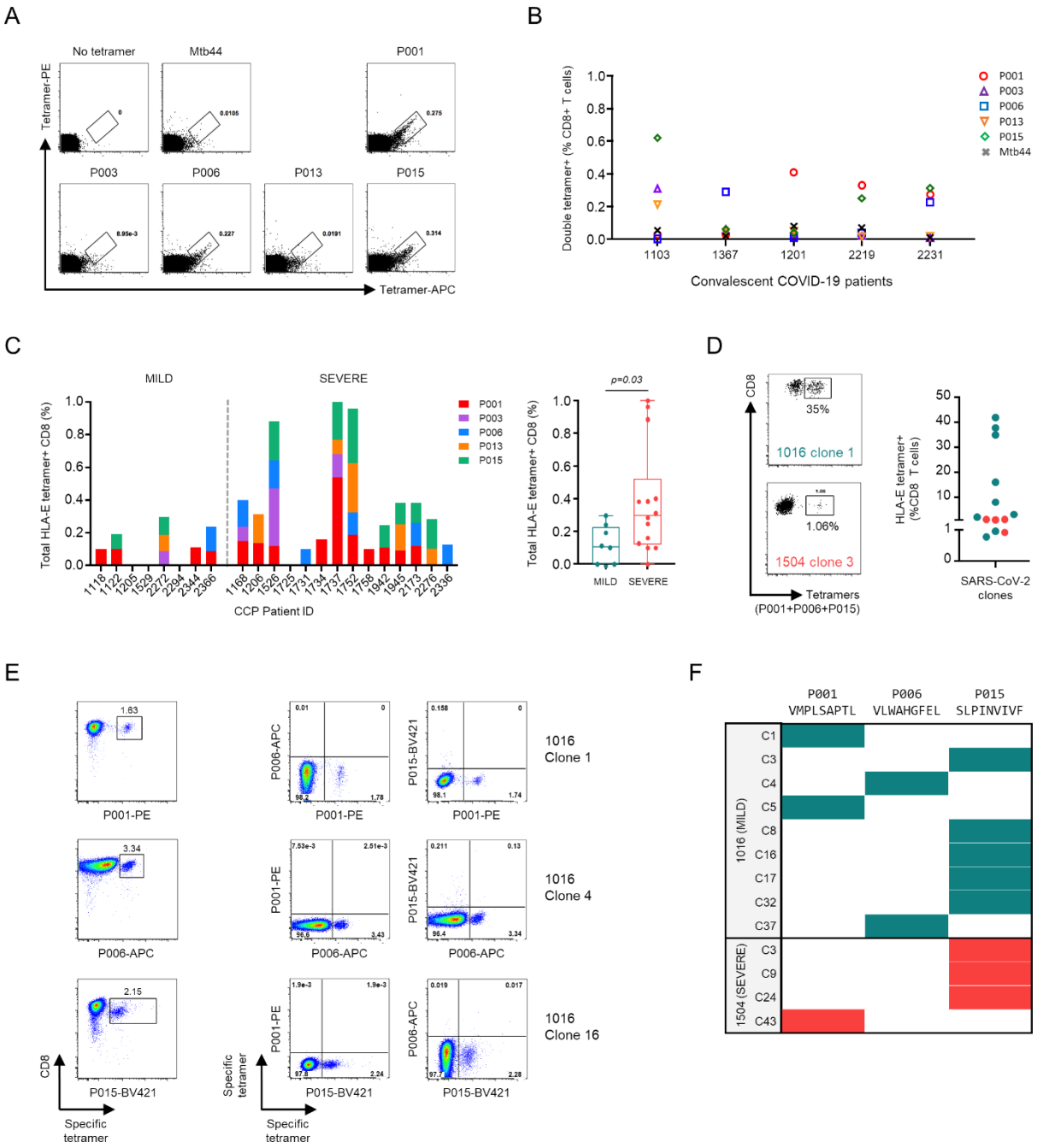

Fig. 2. HLA-E restricted SARS-CoV-2-specific CD8 cells in convalescent COVID-19 patients

A, Using the method of UV exchange, the top 5 HLA-E binding SARS-CoV2 specific peptides (P001, 003, 006, 013 and 015) were introduced into HLA-E to produce fluorescent tetramers. Representative FACs plots of PBMC from convalescent COVID-19 patients co-stained with APC- and PE-conjugated HLA-E tetramers are shown, with peptide specific CD8+ T cells identified as double tetramer positive cells. An HLA-E tetramer exchanged with Mtb44 (RLPAKAPLL), an epitope from *Mycobacterium tuberculosis,* was included as an irrelevant HLA-E tetramer control. **B,** The frequencies of *ex vivo* derived CD8+ tetramer+ cells from 5 convalescent patients

together with the irrelevant Mtb44 tetramer, as assessed by double APC versus PE double staining is summarized. **C,** Tetramer+CD8+ T cell staining for the top 5 HLA-E binding peptides was evaluated in the ISARIC convalescent cohort (n=22). Tetramer+CD8+T cell frequencies were plotted against patient identifiers (left) and disease severity (right). Severe patients, red dots; mild patients, green dots. Significance was calculated using Mann-Whitney test. **D,** Representative flow graphs depicting the tetramer staining of SARS-CoV-2 specific CD8 clones. The frequencies of tetramer+ CD8+ T cells of all 13 clones are displayed. Pt1016 clones, green dots; Pt1504 clones, red dots. **E,** Representative FACS plots demonstrating the tetramer-specificity of individual SARS-CoV-2 CD8 clones evaluated using tetramers tagged with different fluorochromes (P001/PE, P006/APC and P015/BV421) is shown. **F,** A heatmap summarizing the peptide specificity of each CD8 clone is presented, where each row denotes separate CD8 clones, and each column represents individual HLA-E SARS-CoV-2 peptides (P001, P006 or P015). Pt1016 clones in green; Pt1504 clones in red.

Functions of HLA-E restricted SARS-CoV-2-specific CD8+ T cells

The functions of the 13 SARS-CoV-2 specific CD8 clones were assessed by measuring expression of cytokines (IFN-γ, TNF-α, MIP1β; IL-4, IL-13), cytolytic proteins (CD107a/b, Granzyme a/b), activation molecules (CD137) and inhibitory molecules (CTLA-4) following peptide stimulation. We used peptide pulsed HLA-E-transduced K562 cells, an erythroleukemia cell line that lacks endogenous HLA class I [20], as the antigen presenting cells (Fig. S5; Fig. 3A-B). Although the responses were weak, we observed increased IL-13 secretion and activation marker CD137 upregulation for most CD8 clones with peptide stimulation compared to mock, defined by mean fold changes of IL-13 secretion at 2.0 and CD137 expression at 1.65 respectively (Fig. 3A). We further tested four clones with different peptide specificities, which demonstrated strong peptide stimulated CD137 expression and at least one other peptide specific function. We included an additional negative control of the irrelevant HLA-E binding peptide Mtb44 stimulation in the function assay. All four clones gave significantly SARS-CoV-2 peptide specific CD137 upregulation compared to controls, and moreover the responses were significantly blocked by competitive inhibition with the canonical HLA-E binding VL9 signal peptide in two clones 1016C3 and 1504C3, the responses were also blocked in clones 1016C1 and 1016C4, but not significantly (Fig. 3B). Blocking of the CD137 expression by the VL9 peptide confirmed that SARS-COV-2 peptides P001, 006 and 015 were presented by HLA-E.

We also used PMA and Ionomycin as a strong stimulus to assess functions of CD8+ clones for comparison. We noted that the clones from Pt1504, the severe disease donor, produced significantly less IFN-γ, higher IL-13 and expressed elevated CTLA-4 relative to those from Pt1016 (Fig. S4D). However, culture of T cell clones may distort their phenotype and larger numbers of donors would be required to relate their functional potential to disease severity.

The maximal PMA-ionomycin stimulation studies emphasised the weak stimulation signal that was given by peptide pulsed HLA-E-ß2m on K562 cells. This might be a consequence of low affinity of peptide TCR recognition and suboptimal antigen presentation by the K562 cells. Therefore, we asked whether the T cell clones recognise SARS-CoV-2 infected Calu-3 cells, a human respiratory epithelial cell line [39,40]. T cell clones were co-cultured with SARS-CoV-2 [Victoria 01/20 (BVIC01)] infected Calu-3 cells at effector: target (E: T) ratios of 1:1 and 4:1 for 15 hours (Fig. 3C). Two CD8+ T cell clones that were completely negative for tetramer staining, although isolated from a SARS-CoV-2 convalescent patient, were used as controls alongside HLA-E-restricted HIV-1 specific CD8+ T cell clones [31]. We assessed antiviral activity by measuring SARS-CoV-2 replication by measuring intracellular viral RNA levels by RT-qPCR[41]. We confirmed that uninfected Calu-3 cells expressed HLA-E at a comparable level to PBMCs (Fig. S6), making it possible for these cells to present SARS-CoV-2 epitopes to CD8+ T cells. Incubating the HLA-E-restricted SARS-CoV-2 specific clones with the infected Calu-3 cells resulted in significantly reduced levels of viral RNA compared to control clones (Fig. 3C-F). The antiviral activity was dose dependent with greater activity at the higher Effector: Target ratio (Fig. 3E-F). Thus HLA-E restricted SARS-CoV-2 specific T cells were capable of recognizing infected cells and suppressing virus replication.

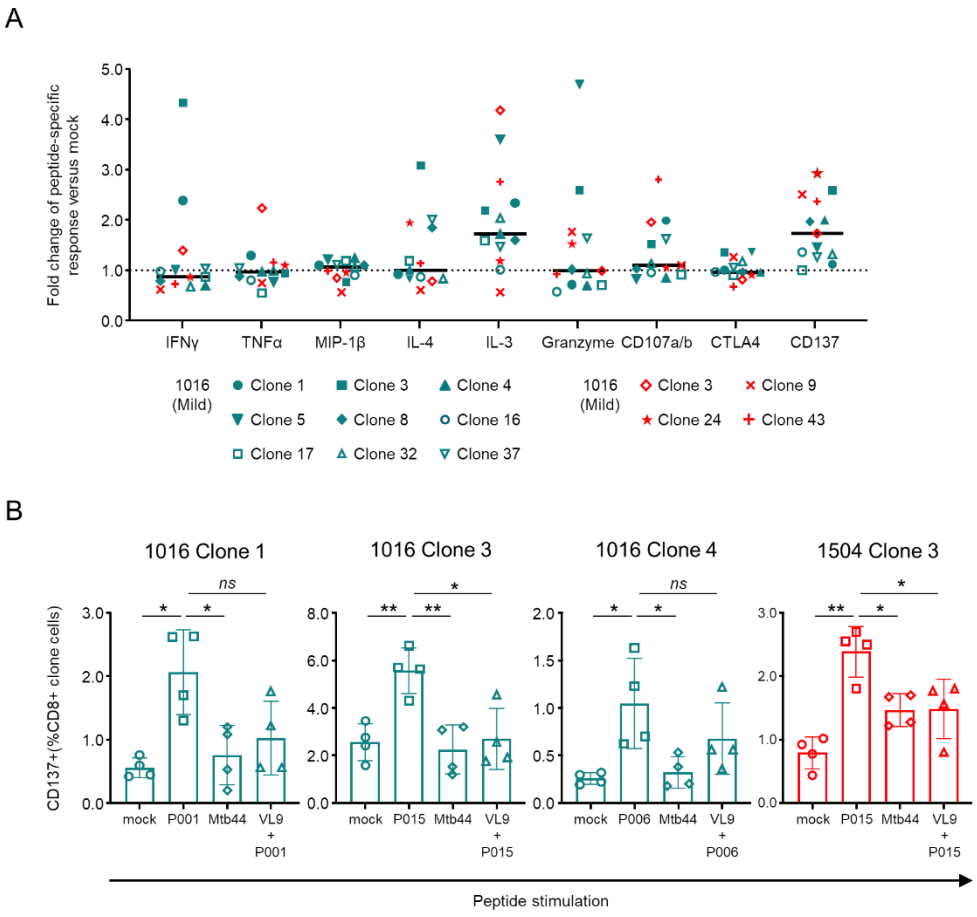
A
Fold change of peptide-specific response versus mock
IFNγ
TNFα
MIP-1β
IL-4
IL-3
Granzyme
CD107a/b
CTLA4
CD137
1016 (Mild)
Clone 1
Clone 3
Clone 4
Clone 5
Clone 8
Clone 16
Clone 17
Clone 32
Clone 37
Clone 24
Clone 43
B
1016 Clone 1
1016 Clone 3
1016 Clone 4
1504 Clone 3
CD137+(%CD8+ clone cells)
mock
P001
P015
P006
Mtb44
VL9 + P001
VL9 + P015
VL9 + P006
Peptide stimulation
C
SARS-CoV-2 MOI 0.01
Calu-3
2 h
CD8+T clones E:T 1:1 or 4:1
15 h
Wash out CD8+T clones
extract Calu-3 RNA and perform RT-qPCR
D
E:T 1:1
1016
1504
irrelevant
Relative SARS-CoV-2 RNA (%)
Calu-3 only
C1
C3
C4
C5
C8
C16
C17
C32
C9
C24
1016 tet-
1504 tet-
RL9HIV P4C2
RL9HIV P12C6
E
p=0.006
Inhibition of SARS-CoV-2 RNA (%)
clones
control
F
E:T 4:1
G
p=0.02

362

Fig. 3. Characterization of the functionalities of HLA-E restricted SARS-CoV-2 specific CD8 clones

A, The upregulation of functional molecules including IFNγ, TNFα, MIP-1β, IL-4, IL-13, CTLA-4, CD107a/b, Granzyme a/b and CD137 on T cell clones following incubation with mock (no peptide) and peptide pulsed HLA-E transduced K562 cells was assessed. Fold change of 9 functional markers assessed with peptide stimulation versus a no peptide control for 13 clones were plotted. **B**, Four responsive clones demonstrating CD137 upregulation were further tested by ICS, with the irrelevant Mtb44 peptide included as an additional negative control. Horizontal line indicates mean plus SD in scatter dot plot. Blockade of CD137 expression by addition of the canonical VL9 signal peptide prior to stimulation with K562-E cells pulsed with SARS-CoV2 peptide is also shown. The data is representative of two independent experiments, analyzed by unpaired t test with Welch's correction. **C-G**, The antiviral capacity of SARS-CoV-2 specific T cell clones was assessed in a viral suppression assay (VSA): intra-cellular viral transcription in Calu-3 infected cells was analyzed using RT-qPCR after co-culture with CD8+ T cell clones. Relative expression of viral transcription normalized to SARS-CoV-2 infected Calu-3 cells is depicted on y-axis. The degree of inhibition, reported as % relative SARS-CoV2 RNA, was compared between clones from patients Pt1016 and Pt1504, patient-derived control T cell clones that did not stain with HLA-E-SARS-CoV-2 tetramers and two HLA-E-restricted clone specific for the HIV-1 Gag RL9 peptide (RL9HIV). The workflow of the VSA is depicted above section C (created in BioRender.com). Viral suppression data at E:T 1:1 (**D-E**) and E:T 4:1 (**F-G**) is presented. Pt1016, green bars/dots; Pt1504, red bars/dots; irrelevant: shade bars/dots. Significance was calculated using Mann Whitney test.

Viral suppression was dependent on the T cell receptors

In order to show that recognition and suppression of SARS CoV-2 infected cells was truly mediated by T cells, TCR Vα and Vβ genes from four responsive clones, fused to murine Cα/Cβ, were transduced using a lentiviral vector into primary CD8+ T cells obtained from healthy donor PBMC [31]. Four T cell clones were selected to represent different peptide specificities either from mild patient 1016 or severe patient 1504: clone 1016C1 (peptide 001), clone 1016C4 (peptide 006), clone 1016C8 (peptide 015) and clone 1504C3 (peptide 015). An irrelevant HLA-E restricted TCR specific for HIV $GAG_{275-283}$ RMYNPTNIL (RL9HIV) [31] was similarly expressed in primary CD8+ T cells from the same donor as an additional negative control for these experiments.

CD8+ T cell transductants were sorted to enrich for a SARS-CoV-2 TCR+ population and stained with anti-mouse Cβ antibody to confirm TCR expression (Fig 4A-B). We noted that some transductants lost TCRs expression during the culture period. A flow based viral suppression assay was developed to study viral infected cells by FACS measurement of Spike expression, providing a way to resolve infected cells beyond a population-based qPCR of viral RNA. Calu-3 cells were infected with SARS-CoV-2 virus [Victoria 01/20 (BVIC01)] at M.O.I of 0.01 and then either cultured alone, co-cultured with SARS-CoV-2 TCR+ transductants or irrelevant HIVGAG TCR transductants. At the end of the coculture, Calu-3 cells were collected and stained with anti-Spike antibody intracellularly. The anti-SARS-CoV-2 activity was quantified by proportional reduction of Spike+ Calu-3 cells when infected Calu-3 were incubated with TCR transductants in comparison to infected Calu-3 cultured alone. CD8+ T cells transduced with four SARS-CoV-2 TCRs reduced Spike+ Calu-3 cells by a mean of 16.2% to 52.6% whilst irrelevant RL9HIV TCR CD8+ transductants showed a mean of 6.3% background reduction. There was a statistically significant difference in inhibition of SARS-

CoV-2 virus replication in Calu-3 cells or killing of infected Calu-3 cells exposed to CD8+ T cells transduced with three out of four SARS-CoV-2 TCRs tested in comparison to HLA-E restricted irrelevant HIVGAG TCR (Fig 4C). The transfer of anti-SARS-CoV-2 reactivity into fresh CD8+ T cells by lentiviral insertion of TCR-Vα and Vβ genes therefore reconfirmed the specificity of the T cell clones.

A

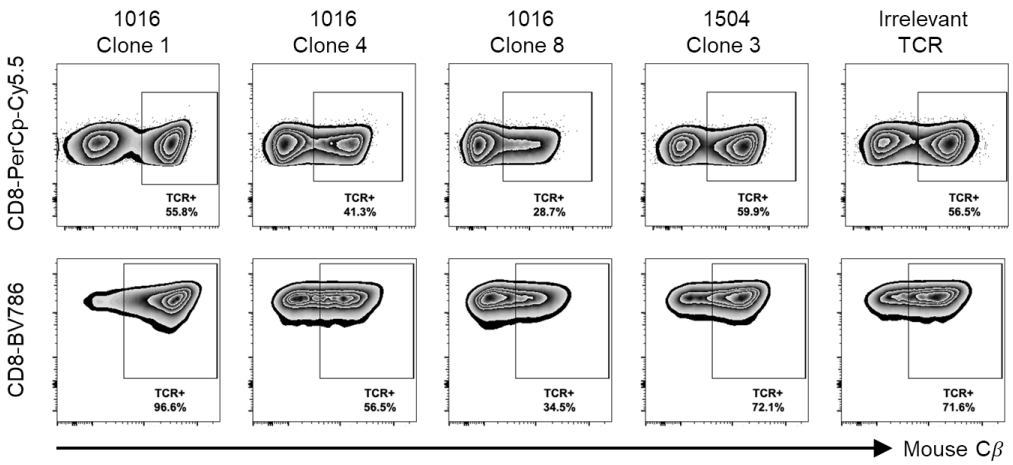
1016 Clone 1
1016 Clone 4
1016 Clone 8
1504 Clone 3
Irrelevant TCR
CD8-PerCp-Cy5.5
CD8-BV786
TCR+ 55.8%
TCR+ 41.3%
TCR+ 28.7%
TCR+ 59.9%
TCR+ 56.5%
TCR+ 96.6%
TCR+ 56.5%
TCR+ 34.5%
TCR+ 72.1%
TCR+ 71.6%
Mouse Cβ

B

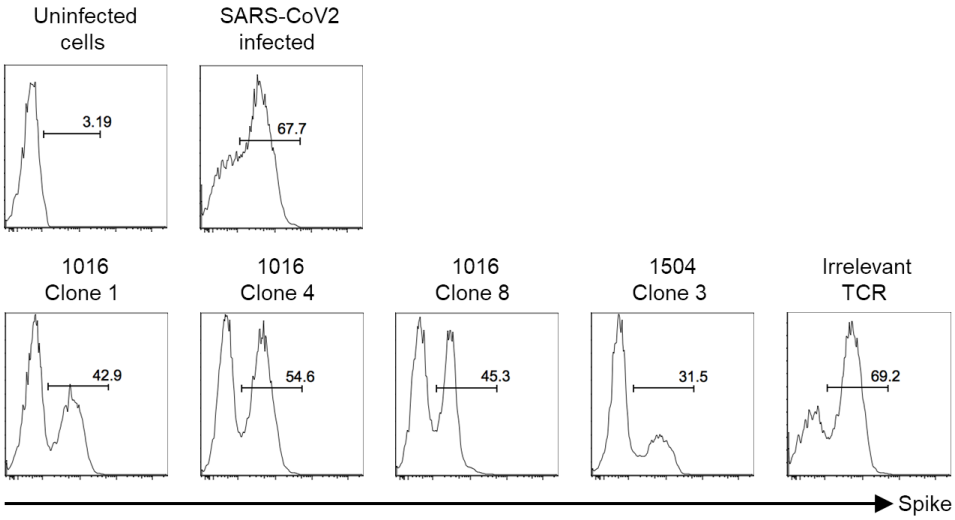
Uninfected cells
SARS-CoV2 infected
3.19
67.7
1016 Clone 1
1016 Clone 4
1016 Clone 8
1504 Clone 3
Irrelevant TCR
42.9
54.6
45.3
31.5
69.2
Spike

C

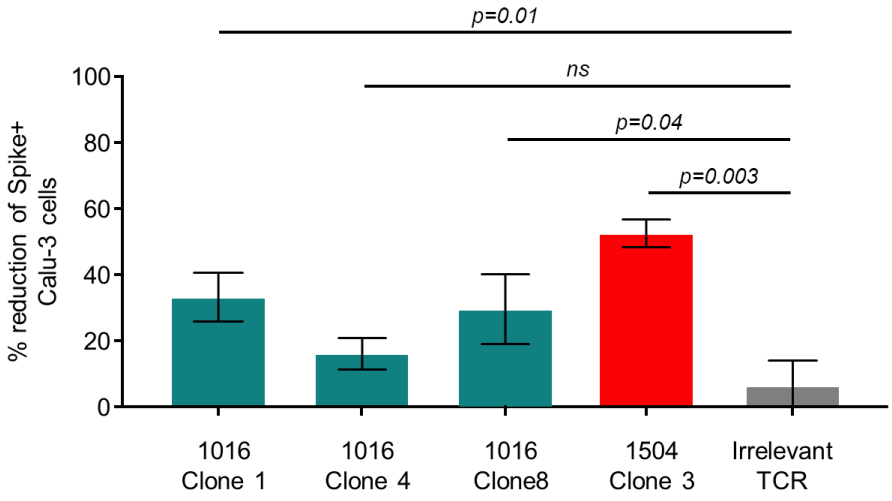
p=0.01
ns
p=0.04
p=0.003
% reduction of Spike+ Calu-3 cells
100
80
60
40
20
0
1016 Clone 1
1016 Clone 4
1016 Clone8
1504 Clone 3
Irrelevant TCR

Fig. 4. Function analysis of primary CD8+ T cells transduced with SARS-CoV2-specific TCRs

Four SARS-CoV2 TCRs and an irrelevant HLA-E restricted TCR specific for HIV $GAG_{275-283}$ RMYNPTNIL (RL9HIV) were transduced into primary CD8+ T cells. **A** top: CD8+ transductants were stained with anti-mouse Cβ antibody, anti-CD8/CD3/CD4 and Live/Dead Fixable Aqua. Mouse Cβ+/CD8+ transductants were sorted and expanded in IL-2/IL-15 media for 17 days. Bottom: Cβ staining was repeated following T cell expansion (as described above). **B** CD8+ transductants were cocultured with SARS-CoV2-infected Calu-3 at E:T ratio of 3:1 for 48hrs. The number of transduced T cells added to the coculture were normalized according to the frequency of mouse Cβ+ CD8+ T cell staining. SARS-CoV2-infected Calu-3 were quantified by intracellular anti-Spike staining. **C** Percentage of reduction of Spike+ cells is shown (calculated as described in Material and Methods). The data shown represents 3 independent experiments. Horizontal lines indicate the mean values. Statistical analysis was performed using unpaired t test with Welch's correction.

SARS-CoV-2 infection perturbs HLA-E and HLA-I expression

Finally, we investigated whether HLA-E restricted T cell responses were influenced by SARS-CoV-2 induced downregulation of HLA-I expression [42]. We monitored infection by quantifying expression of the viral encoded Spike glycoprotein and observed an increasing frequency of Spike positive cells over time, consistent with a spreading infection (Fig. 5A-B). We confirmed that Spike expression was dependent on virus replication, as treating cells with Remdesivir (RDV), a ribonucleotide inhibitor of RNA-dependent RNA polymerase, ablated Spike expression (Fig. 5A-B). SARS-CoV-2 infected Spike positive cells showed an increase in cell surface HLA-E expression and reduced levels of HLA-Ia compared to uninfected cells and this phenotype was eliminated by RDV treatment (Fig. 5C, Fig. S7). Infecting the cells with differing amounts of virus (MOI of 0.1 and 1) showed a dose-dependent virus modulation of both surface and total HLA-E and HLA-I expression (Fig. 5D-F). At 48 hours post-infection (hpi), when cells infected at MOIs of 0.01 were evaluated as cell cultures infected at higher MOI exhibited substantial cytopathic effects at this time point, HLA-I expression was significantly reduced in spike positive compared to negative cells. In contrast, HLA-E expression was unchanged (Fig. 5G, H). Furthermore, we noted a time-dependency in virus perturbation of HLA expression (Fig. 5F). We obtained similar results using an independent lung epithelial A549 cell line engineered to express ACE2 (A549-ACE2) [43]. We noted similar infection rates with comparable Spike expression over time with similar perturbations in HLA-I and HLA-E expression (Fig. S8).

To assess whether HLA-I downregulation occurs in SARS-CoV-2 infected primary epithelial cells, we infected primary reconstituted human airway epithelial cells (MuciAir^{TM}) with SARS-CoV-2 mNeonGreen reporter virus [44] at M.O.I of 0.1. Infected epithelia cells were identified as green fluorescent cells. HLA-E and HLA-I expression were evaluated at 48

hours post-infection (hpi) by surface staining with anti-HLA-A, B, C antibody W6/32 and anti-HLA-E antibody 3D12. We observed a substantial reduction of HLA-class I expression in infected epithelia cells compared to un-infected cells, whilst HLA-E expression was only marginally reduced (Fig 5I).

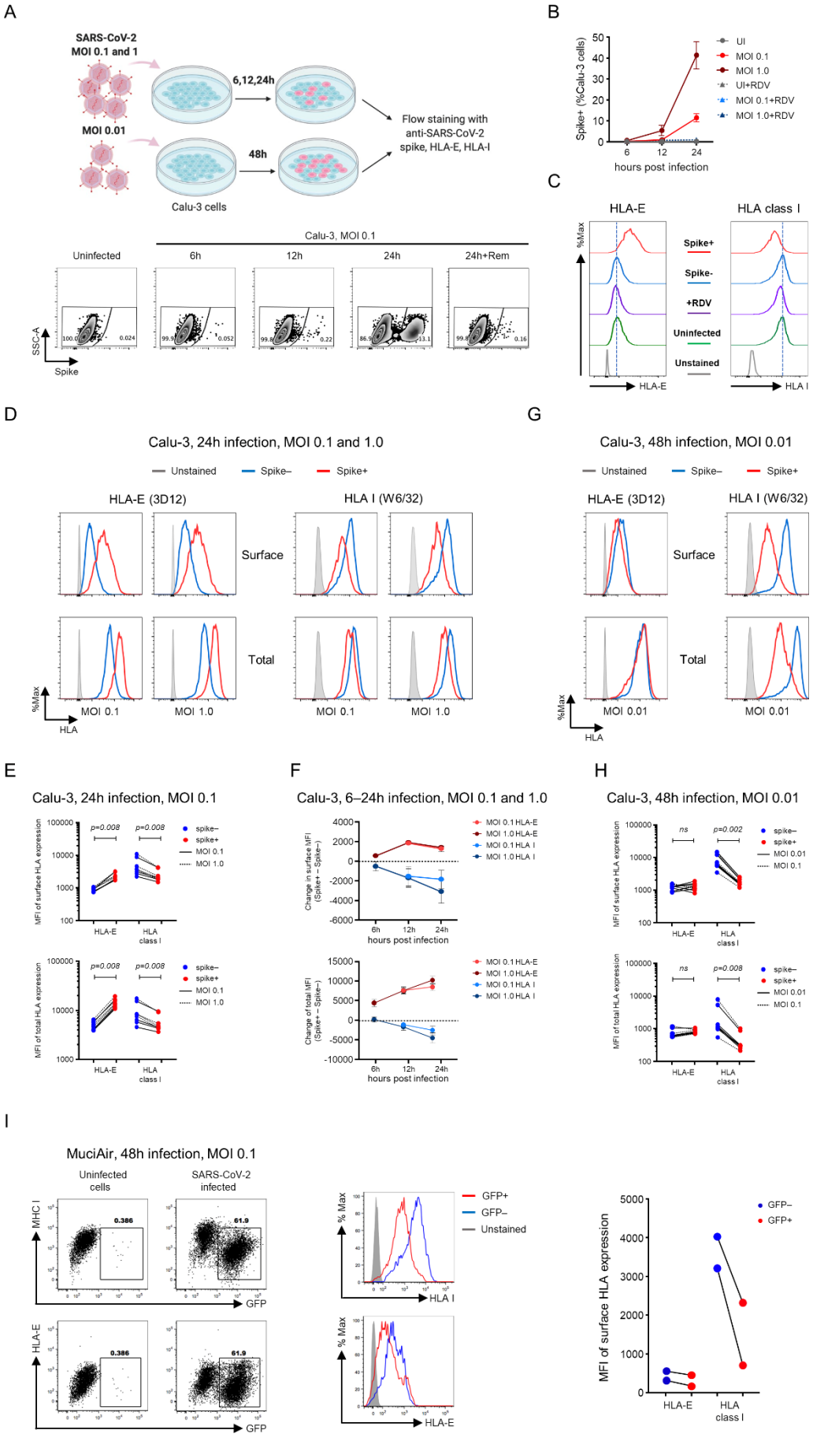
A
SARS-CoV-2
MOI 0.1 and 1
MOI 0.01
6,12,24h
48h
Calu-3 cells
Flow staining with
anti-SARS-CoV-2
spike, HLA-E, HLA-I
Calu-3, MOI 0.1
Uninfected
6h
12h
24h
24h+Rem
SSC-A
Spike
B
Spike+ (%Calu-3 cells)
hours post infection
UI
MOI 0.1
MOI 1.0
UI+RDV
MOI 0.1+RDV
MOI 1.0+RDV
C
HLA-E
HLA class I
%Max
Spike+
Spike-
+RDV
Uninfected
Unstained
HLA-E
HLA I
D
Calu-3, 24h infection, MOI 0.1 and 1.0
Unstained
Spike–
Spike+
HLA-E (3D12)
HLA I (W6/32)
Surface
Total
%Max
MOI 0.1
MOI 1.0
HLA
G
Calu-3, 48h infection, MOI 0.01
Unstained
Spike–
Spike+
HLA-E (3D12)
HLA I (W6/32)
Surface
Total
%Max
MOI 0.01
HLA
E
Calu-3, 24h infection, MOI 0.1
MFI of surface HLA expression
MFI of total HLA expression
p=0.008
spike–
spike+
MOI 0.1
MOI 1.0
HLA-E
HLA class I
F
Calu-3, 6–24h infection, MOI 0.1 and 1.0
Change in surface MFI (Spike+ – Spike–)
Change of total MFI (Spike+ – Spike–)
MOI 0.1 HLA-E
MOI 1.0 HLA-E
MOI 0.1 HLA I
MOI 1.0 HLA I
hours post infection
H
Calu-3, 48h infection, MOI 0.01
MFI of surface HLA expression
MFI of total HLA expression
ns
p=0.002
p=0.008
spike–
spike+
MOI 0.01
MOI 0.1
HLA-E
HLA class I
I
MuciAir, 48h infection, MOI 0.1
Uninfected cells
SARS-CoV-2 infected
MHC I
HLA-E
GFP
0.386
61.9
% Max
GFP+
GFP–
Unstained
HLA I
HLA-E
MFI of surface HLA expression
GFP–
GFP+
HLA-E
HLA class I

Fig. 5. HLA-E and HLA-I dysregulation in Calu-3 cells and primary airway epithelial cells upon SARS-CoV-2 infection

A-B, Replication dynamics of SARS-CoV-2 in Calu-3 cells was assessed by anti-SARS-CoV-2 spike antibody staining following SARS-CoV-2 virus infection at different MOIs and timepoints following infection: MOI 1 and 0.1 at 6, 12, 24 hpi, or MOI 0.01 at 48hpi. **A**, The infection and evaluation workflow is depicted (upper diagram, created in BioRender.com). Representative graphs depict $Spike^+$ cells, assessed by intracellular (ICS) staining at a MOI 0.1 (represented as SSC versus ICS). 2 hours after viral infection, Remdesivir (Rem) was added. **B**, SARS-CoV-2 infection kinetics for Calu-3 cells at the indicated timepoints is depicted. MOI 1, cayenne; MOI 0.1, red; MOI 1 with Remdesivir treatment, ocean; MOI 0.1 with Remdesivir treatment, blue; uninfected (UI), grey. Remdesivir addition, triangle. The mean ±SEM of 4 biological repeats is shown. **C**, HLA-E and HLA-I surface expression, assessed by anti-3D12 and anti-W6/32 staining respectively (reported as the Median Fluorescent Intensity (MFI)), for each condition at 24hpi and MOI 0.1 is depicted. Spike+, red; Spike-, blue; Remdesivir, purple; Uninfected control, green; Unstained, grey. **D**, Representative histograms (MOI 0.1 and 1) denote HLA expression (MFI) of Spike+ and Spike- cells on the surface (upper panel) and in total (lower panel) at 24hpi. Spike+, red; spike-, blue; unstained control, grey. **E**, The MFI of HLA expression of Spike+ and Spike- Calu-3 cells was compared. MOI 0.1, solid line; MOI 1, dash line; spike+, red; spike-, blue. Statistical analysis of the data were performed using Wilcoxon rank test. **F**, HLA-E and HLA-I expression in spike+ versus spike- Calu-3 cells change dynamically with time. MOI 0.1, red (HLA-E) and blue (HLA-I); MOI 1, cayenne (HLA-E) and ocean (HLA-I). The mean ± SEM of 4 biological repeats is shown **G**, Representative histograms (MOI 0.01) denote HLA expression of spike+ and spike- cells on the surface (upper panel) and in total lower panel) at 48hpi. Statistical analysis of the data was performed using Wilcoxon rank test. **H**, MFI of HLA expression of Spike+ and Spike- Calu-3 was compared. Spike+, red; spike-, blue. **I** primary reconstituted human airway epithelia cells (MuciAir^{TM}, Epithelix) were infected with the mNEONGreen reporter SARS-CoV-2 viral strain, pSC2-Rep-Wu-p-RL-6NG (ORF6 mNeonGreen) at M.O.I of 0.1. Infected cells were identified as green fluorescent cells. HLA-E and HLA-I expression were evaluated at 48 hours post-infection by surface staining with anti-HLA-A, B, C antibody w6/32 and anti-HLA-E antibody 3D12. Data shown is representative of two independent experimental assays.

Comparison of functional activities of HLA-E restricted and HLA-A*2402 restricted CD8+ T cell clones on SARS-CoV2 virus-infected Calu-3 cells.

The observation that SARS-CoV-2 infection reduced HLA-class Ia surface expression prompted us to test whether CD8+ T cell responses were affected. As Calu-3 cells express HLA-A*2402 we selected a SARS-CoV2 specific CD8+ T cell clone specific for the Spike peptide $S_{1208-1216}$ QYIKWPWYI: (QI9) to compare the function of classical CD8+ T cells, these T cells were stimulated by pulsing uninfected or SARS-CoV-2 infected Calu-3 cells with their cognate peptide and activity measured by assessing TNF-α and CD107a/b expression. We detected TNF-α secretion and increased CD107a/b expression in Spike QI9 pulsed uninfected Calu-3 cells (Fig. S9A). However, when the A24 restricted T cell clone cells were stimulated by SARS-CoV-2 infected Calu-3 cells, with or without pulsing with Spike QI9 peptide, both TNF-α and CD107a/b responses were significantly reduced (Fig. S9B-C).

Next, we compared the anti-viral activity of three HLA-E restricted T cell clones along with the A24 Spike clone. Calu-3 cells were infected with SARS-CoV-2 [Victoria 01/20 (BVIC01)] at M.O.I of 0.1 for 1 hour and cultured with CD8+ T cell clones at an E:T ratio of 3:1. At end of 48 hours coculture, CD8+ T cells were washed off and Calu-3 cells were trypsinized to release them from the tissue culture wells and stained for intracellular Spike expression (Fig. 6). The HLA-E restricted T cell clone clones 1016C1, 1016C4 and 1504C3 showed mean inhibition of 40%, 29.1% and 65.2% respectively, while the HLA-A*2402 restricted Spike specific clone showed 26.9%. inhibition. However only clones 1106C1 and 1504C3 showed statistically significant higher inhibition than the HLA A*2402 restricted control clone (Fig.6).

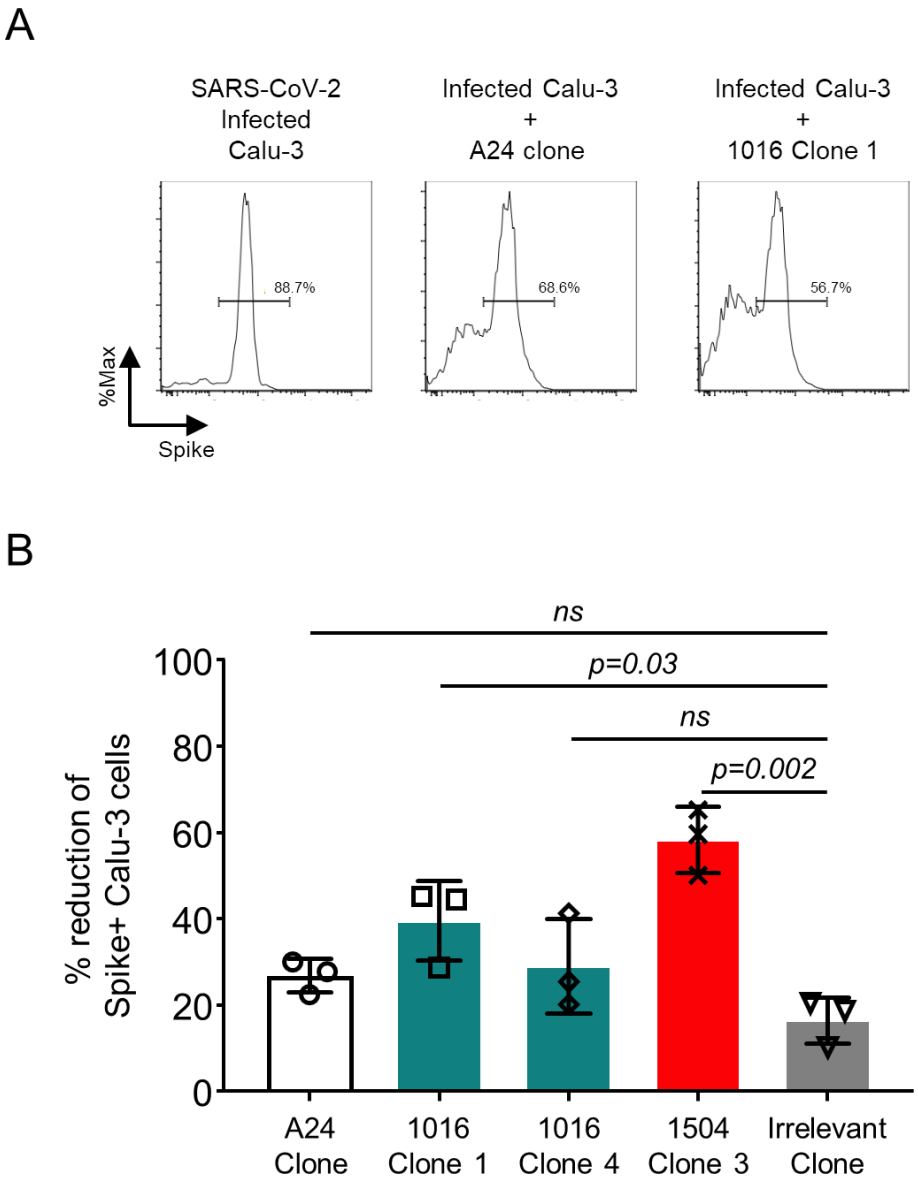

Fig. 6. Anti-SARS-CoV2 activities of HLA-A24 restricted and HLA-E restricted CD8+ T cell clones

A. HLA-E CD8+ T cell clones or A24 Spike CD8+ T cell clone were cocultured with SARS-CoV2-infected Calu-3 at E:T ratio of 3:1 for 48hrs. SARS-CoV2-infected Calu-3 were quantified by intracellular anti-Spike antibody staining. **B** Percentage of reduction of Spike+ cells were shown (calculated as described in Material and Methods). Data shown is from 3 independent experiments. Horizontal line indicates mean plus SD in scatter dot plot. Statistical analysis was performed using unpaired t test with Welch's correction.

DISCUSSION

Several studies have demonstrated the presence and potential importance of the CD8+ T cell response in SARS-CoV-2 infection [21,23-25,45-51]. There has been much interest in their possible role in cross-strain protection and amelioration of severe disease [48]. However, it is also becoming apparent that the virus may be able to partially or completely evade these immune responses. One immune evasion mechanism is mediated by ORF6 through targeting MHC Class I antigen-presenting pathway [52]. ORF6 hampers type II interferon mediated STATI signalling, resulting in MHC class I transactivator suppression both transcriptionally and functionally. Two other studies also provide a potential explanation for the downregulation of class I HLA in SARS CoV-2 infected cells. Zhang et al [42] show that the virus ORF8 gene product targets HLA-class I molecules for autophagy and degradation, thereby reducing total HLA-I expression. In addition, Hsu et al [53] showed that SARS CoV-2 infection rapidly shuts down host protein translation, a process dependent on NSP14. This mechanism is likely to impact on classical antigen processing where peptides transported by the transporter associated with antigen processing (TAP) from the cytosol to the peptide loading complex in the ER, bind to newly synthesised HLA class I molecules, which then traffic rapidly to the cell surface. In contrast, HLA-E is normally retained in the ER [4,54] and could continue to bind pathogen peptides when protein translation is blocked [14,15]. Furthermore, Munnur D et al [55] have shown that SARS-CoV-2 viruses antagonize ubiquitin-like protein ISG15 (interferon-stimulated gene 15) to downregulate both MHC-Class I and Class II expressions on SARS-CoV-2 infected macrophages and triggers aberrant macrophage-dependent immune responses.

Here we identified five peptides in SARS-CoV-2 that bind to HLA-E with sufficient stability to prepare HLA-E-peptide tetramers. These were used to show that convalescent Covid-19 patients had circulating blood HLA-E restricted T cells which were present at similar levels to

previously described classical virus specific CD8+ T cells [21-26]. We generated T cell clones showing antigen specific responses to peptide pulsed presenting cells and an ability to suppress virus replication in the Calu-3 lung epithelial cell line. Similar results were obtained when the TCR was transferred using lentiviral transduction to primary CD8+ T cells. It is noteworthy that the clone and TCR-transductant T cell responses measured as the numbers of T cells responding in short term peptide stimulation assays were quite weak, though positive, whereas the virus suppression measured on infected target cells in a 48-hour assay was relatively strong. This probably reflects low affinity binding of the peptide to HLA-E and low affinity TCR receptor binding to the complex. Besides its lack of polymorphism, HLA-E is unusual in remaining associated with ß2 microglobulin in the absence of peptide and remaining peptide receptive [15,16,18], in contrast to most classical HLA class I molecule which fall apart in the absence of specific peptide. Thus HLA-E can seemingly bind lower affinity peptides sufficiently well to prime and maintain T cell responses. However, the T cell responses appear to be low affinity with relatively low tetramer binding We suggest that these low affinity responses could be well suited to make sustained attacks on virus infected cells without the risk of activation induced T cell death.

A further advantage of HLA-E is its resistance to virus mediated downregulation. Thus, while classical HLA class I was markedly downregulated in SARS-CoV-2 infected cells, HLA-E was not. As a result, the surface levels of HLA-Ia and HLA-E on infected Calu-3 and primary bronchial epithelial cells were similar. The virus induced downregulation of HLA-A*2402 greatly affected specific peptide presentation. On infected Calu-3 cells, virus suppression *in vitro* was similar for both. If the HLA-A*2402 restricted T cell clone is representative of other classical T cell responses, this would suggest that HLA-E restricted T cells could to be as effective as classical CD8+ T cells in controlling infection in vivo, particularly given the

relatively high levels of HLA-E expression in the lower respiratory tract (https://www.proteinatlas.org/ENSG00000204592-HLA-E/tissue).

HLA-E restricted T cells have only rarely been described. However, they are abundant in the blood in mycobacterial infections in humans[7-10] and after immunisation with a rhesus cytomegalovirus vaccine in monkeys[7]. Some of the rarity might result from a lack of suitable reagents for detection, but a common feature to these different infections could be downregulation (CMV and SARS-CoV-2) or bypassing (mycobacteria [15]) of classical class I MHC antigen presentation. The former could favour MHC-E where competition with classical MHC is reduced allowing alternative processing pathways to come into play[14]

The similar levels of HLA-E and HLA-Ia on infected cells could explain why the classical T cell responses are present at similar levels to the HLA-E restricted T cell frequencies seen here, after SARS CoV-2 infection[21-26]. The relative protective activities of HLA-E restricted compared to HLA-Ia restricted T cells remain to be determined, but it is likely that the normal balance, which is strongly in favour of classically restricted T cells, is disturbed in SARS-CoV-2 infection and that HLA-E-restriction could be important in this specific setting. If so, then induction of HLA-E restricted T cell responses by vaccines focused on the universal epitopes could be an attractive possibility.

Materials and Methods:

Study Design

The project aimed to elucidate the presence of HLA-E restricted CD8 response in convalescent COVID-19 patients using HLA-E tetramers in complex with 5 SARS-CoV-2 derived peptides. HLA-E restricted CD8+ T cell clones generated from the patients in response to these peptides demonstrated antiviral activity against SARS-CoV-2 infected Calu-3 cells. SARS-CoV-2 infection downregulated classical HLA-I expression *in vitro* while HLA-E expression

656 remained unaltered, thereby potentially explaining why increased frequencies of HLA-E
657 restricted T cells against SARS-Co2-derived epitopes exist *in vivo*.
658
659 **Study participants and ethical approvals**
660 Five convalescent COVID-19 patients in the pilot study were enrolled in the John Radcliffe
661 Hospital in Oxford described previously [23] while 22 convalescent COVID-19 patients were
662 recruited from University of Liverpool from the International Severe Acute Respiratory and
663 Emerging Infections Consortium (ISARIC)/World Health Organization (WHO) Clinical
664 Characterisation Protocol for severe emerging infection UK (CCP-UK) cohort study (Study
665 registration ISRCTN66726260 https://doi.org/10.1186/ISRCTN66726260).
666 For clinical stratification of these patients, mild disease is defined as no oxygen requirement
667 and no admission onto the intensive treatment unit (ITU) survived to discharge and severe
668 disease is defined as any requirement for oxygen, or receipt of Continuous Positive Airway
669 Pressure (CPAP) or high flow oxygen, admission onto the ITU or death.
670 The study was approved by South Central–Oxford C Research Ethics Committee in England
671 (reference: 13/SC/0149) and Scotland A Research Ethics Committee (reference: 20/SS/0028)
672 and World Health Organization Ethics Review Committee (RPC571 and RPC572l; 25 April
673 2013). All participants have signed the informed consent.
674
675 **Peptides**
676 Synthetic 9 amino acid SARS-CoV-2 derived peptides and HLA-B leader sequence peptide
677 VMAPRTVLL (VL9), were synthesized by Genscript (>85% purity). A UV-labile HLA-B
678 leader-based peptide (VMAPRTLVL) incorporating a 3-amino-3-(2-nitrophenyl)-propionic
679 acid residue substitution at position 5 (J residue) was synthesised by Dris Elatmioui at Leiden

University Medical Centre, The Netherlands. Lyophilized peptides were initially reconstituted to 200mM or 100mM in DMSO and aliquoted for cryopreservation at -80℃ until further use.

Protein expression, purification and refolding

The details of HLA-E heavy chain expression, inclusion body preparation-solubilisation, refolding and final purification were performed according to protocols have been previously described [5,7,11,12,31].

Differential scanning fluorimetry

The thermal stability of no-peptide and peptide-loaded HLA-E was determined by differential scanning fluorimetry (DSF) using Prometheus NT.48 Series instrumentation (Nanotemper). Assay design was based on a previously published method [56]. In brief, 0.45 μg/μL of HLA-E was incubated with 100M excess peptide in a 20μL final volume of 50mM Tris pH 7, 150mM NaCl buffer for 30 minutes. Following incubation, approximately 20μL of individual samples were split between two Prometheus NT.48 Series nanoDSF Grade Standard Capillaries (Nanotemper, Munich, Germany) and transferred into a capillary sample holder. Excitation power was pre-adjusted to obtain a range between 8000 and 15,000 Raw Fluorescence Units for fluorescence emission detection at 330 nm and 350 nm. A thermal ramp of 1 °C/min from 20 °C to 95 °C was applied. Thermal melt data calling was automatically generated using the analysis software within PR.ThermControl software version 2.1.5.

Cell lines and primary cells

The MHC-I null cell line K562 transfected with HLA-E*01:03 (K562-E line) was kindly provided by Thorbald van Hall (LUMC) [20] . Calu-3 were provided from Anderson Ryan (Oncology Department, University of Oxford) and A549-ACE2 cells were provided by Alfredo

Castello (CVR, University of Glasgow) [41]. Primary reconstituted human airway epithelia cell MuciAir™ was purchased from EPITHELIX (Geneve, Switzerland). PBMCs were isolated from healthy donor leukapheresis cones obtained pre-UK COVID-19 pandemic (March 2019 to Jan 2020, NHS Blood and Transplant, UK) by density gradient separation.

Single Chain Trimers

Single chain trimer constructs were made and tested as previously described [7,11]. Expression relative to the control construct (which encoded the peptide VMAPRTLLL) was calculated from median fluorescent intensity (MFI) of the transfected cells, corrected by subtracting the MFI of mock transfected cells.

HLA-E binding peptide-exchange ELISA assay

A sensitive HLA-E binding ELISA assay was performed as described with minor optimization [15,16]. Briefly, refolded HLA-E proteins (0.5μM) preloaded with a labile VL9 variant peptide (7MT2) was incubated in the presence of excess SARS-CoV-2 derived peptides at 100μM. The exchange reaction took place overnight in buffer comprising 400mM L-arginine monohydrochloride, 100mM Tris, 5mM reduced glutathione, 0.5mM oxidized Glutathione and 2 mM EDTA. The reaction was diluted 1:100 in phosphate buffered saline (PBS)-2% bovine serum albumin (BSA) and 50 μL was added to ELISA plates pre-coated with 20μg/mL anti-human HLA-E mAb (3D12, Biolegend). After 1 hour, plates were washed with PBS/0.05%Tween-20 and incubated with 2μg/mL anti-human β2M horseradish peroxidase (HRP)-conjugated IgG antibodies for 30 mins. Following subsequent wash steps, 50μL enhancement reagent (Dako EnVision, diluted in PBS/2%BSA with 1% normal mouse serum) was added to amplify the HRP signal. 100μL TMB substrate was added for development and the reaction was terminated with 100μL STOP Solution. Absorbance at 450nm was read using

a FLUOstar OMEGA reader. Three independent peptide-exchange reactions per peptide were included per test, with 2 duplicates from each reaction tested in the ELISA assay. Each run comprised VL9 positive control and a peptide-free no-rescue control to normalize the background and to express the binding affinity as %VL9. The HLA-E binding rankings were calculated as (average tested peptide signals-average DMSO signals)/ (average VL9 signals-average DMSO signals).

HLA-E tetramers generation and staining of $CD8^+$ T cells

UV peptide exchange HLA-E*01:03-biotinylated monomers were conjugated to streptavidin-bound PE, APC or BV421 at a Molar ratio of 4:1 as described [5]. Conventional tetramers were additionally prepared for P001 (VMPLSAPTL). PBMCs from COVID-19 patients were stained with conventional or UV-exchanged tetramers at 0.5ug per $1x10^6$ cells for 45 minutes at room temperature (RT) in the dark. Upon washing with PBS, cells were subsequently stained with Live/Dead Fixable Aqua and flow antibodies to surface markers for 20 min at RT in the dark. Alternatively, the modified wash procedure was taken as the wash step before surface antibody staining was omitted as indicated. Cells were then washed and fixed with 2% paraformaldehyde, and then acquired using a LSR Fortessa (BD Biosciences). The data were analyzed using FlowJo software v10.4 (Tree Star).

Live cell sorting and cloning of HLA-E tetramer positive $CD8^+$T cells

PBMCs from convalescent patients were stained with HLA-E tetramers initially. Cells were subsequently washed with PBS and stained with Live/Dead Fixable Aqua, anti-CD3–APC-Cy7, anti-CD4–PerCP-Cy5.5, anti-CD8-BV421, anti-CD94-FITC and anti-CD56-BV510 for 30 mins at RT in the dark. $CD3^+CD4^-CD56^-CD94^-CD8^+Tetramer^+$ T cells were live sorted using FACSAria III (BD Biosciences). Sorted cells were seeded into 384-well plates at 0.4

cells per well with irradiated (45 Gy) allogeneic feeder cells (3 healthy donors, $2x10^6$ cells/mL) stimulated with PHA (1μg/mL) and IL-2 (500 U/mL) cultured in complete media (CM) containing RPMI 1640, 10% AB human sera (UK National Blood Service), 1% penicillin/streptomycin, 1% glutamine, 1% sodium pyruvate, 1% non-essential amino acids, 0.1% beta-mercaptoethanol. 12 days later, T cell clones were further expanded with feeder cells and PHA/IL-2. Tetramer positivity was tested using HLA-E tetramers (APC-, BV421- or PE-conjugated) and anti-CD3-APC-Cy7, anti-CD8-BV421, and Live/Dead Fixable Aqua. Functions of CD8 clones were subsequently assessed using intracellular staining described below.

HLA-A24 restricted SARS-CoV2 specific CD8+ T cell clone ($Spike_{1208-1216}$ QYIKWPWYI) was kindly provided by Professor Tao Dong, MRC Human Immunology Unit, Weatherall Institute of Molecular Medicine, Oxford University.

Functional assessment of SARS-CoV-2 specific $CD8^+$T cells

To evaluate the functions of CD8 clones, cells were rested in CM before coculture with a genetically modified K562 cell line (HLA-E-expressing, classical HLA-I null) incubated overnight with peptides (50μM) at 27°C. The coculture was incubated at the CD8: K562 ratio of 1:3 for 9 hours. For maximal functionality testing, CD8 clones were also independently treated with PMA/Ionomycin. Brefeldin A (5μg/ml) and GolgiStop (5μg/ml) were added after 1 hour during incubation. Anti-CD107a-BV421 and anti-CD107b-BV421 were supplemented at beginning of coculture. Cells were stained with Live/Dead Fixable Aqua and flow antibodies surface markers (anti-human CD3 and anti-human CD8) in PBS, and then fixed and permeabilized with Cytofix/Cytoperm (BD Biosciences). Intracellular staining (ICS) was performed with fluorochrome-conjugated antibodies against TNFα, IFN-γ, MIP-1β, IL-4, IL-

13, CTLA-4 and CD137 in Permwash solution. Cells were acquired on a LSRFortessa (BD Biosciences) and analyzed using FlowJo v10.4 (Tree Star).

Peptide specific function of HLA-A24 restricted SARS-CoV2 specific CD8+ T cell clone ($Spike_{1208-1216}$ QYIKWPWYI) was analyzed by stimulation with un-infected Calu-3 or SARS-CoV2-infected Calu-3 pulsed with A24 peptide at final concentration of 20μM.

TCR sequencing

Total RNA of CD8 clones was extracted using a RNeasy Plus Mini Kit (Qiagen). TCR libraries using around 100ng RNA were prepared using a SMARTer Human TCR a/b Profiling Kit (Takara Bio) according to the manufacturer instructions based on SMART [29] and 5'RACE techniques [30]. Subsequently, full length TCR alpha and beta chains were sequenced using a Miseq Reagent Kit v3 (600-cycle) on an Miseq sequencer (Illumina). Raw BCL files were converted to FASTQ format using bcl2fastq (v2.20.0.422). TCR sequences were then reconstructed using MiXCR (v3.0.13) [57], using the mixcr analyze amplicon command, and only productive TCRs were included. MiXCR output files were parsed into R (v4.0.1) using tcR (v2.3.2). TCRs were filtered based on clone counts to retain only 1α1β or 2α1β paired TCRs for each clone. Clonality was confirmed by the uniqueness of TCR sequences, where each clone showed only one TCR β chain (Table 1).

SARS-CoV-2 virus

The SARS-CoV-2 viral strain, Victoria 01/20 (BVIC01), was provided by PHE Porton Down after the provision from the Doherty Centre Melbourne, Australia [58].

The mNEONGreen reporter SARS-CoV-2 viral strain, pSC2-Rep-Wu-p-RL-6NG (ORF6 mNeonGreen) was provided by Professor Andrew Davidson, School of Cellular and Molecular Medicine, University of Bristol, UK. The recombinant virus was generated using

804 a SARS-CoV-2 (Wuhan isolate) reverse genetics system utilizing the "transformation-
805 associated recombination in yeast" approach [44]. 11 cDNA fragments with 70 bp end-terminal
806 overlaps which spanned the entire SARS-CoV-2 isolate Wuhan-Hu-1 genome (GenBank
807 accession: NC_045512) and replaced the ORF6 coding sequence with that of a codon
808 optimised mNeonGreen were produced by GeneArt™ synthesis (Invitrogen™,
809 ThermoFisher) as inserts in sequence verified, stable plasmid clones. The 5′-terminal cDNA
810 fragment was modified to contain a T7 RNA polymerase promoter and an extra "G"
811 nucleotide immediately upstream of the SARS-CoV-2 5′ sequence, whilst the 3′-terminal
812 cDNA fragment was modified such that the 3' end of the SARS-CoV-2 genome was
813 followed by a stretch of 33 "A"s followed by the unique restriction enzyme site AscI. The
814 inserts were amplified by PCR using a Platinum SuperFi II mastermix (ThermoFisher) and
815 assembled into a full-length SARS-CoV-2 cDNA clone in the YAC vector pYESL1 using a
816 GeneArt™ High-Order Genetic Assembly System (Invitrogen™, ThermoFisher) according
817 to the manufacturer's instructions. RNA transcripts produced from the YAC clone by
818 transcription with T7 polymerase were used to recover infectious virus. Whole genome
819 sequencing confirmed the virus sequence. The virus was propagated in VeroE6/TMPRSS
820 cells grown in infection medium (Eagle's minimum essential medium plus GlutaMAX
821 (MEM, Gibco) supplemented with 2% FBS and NEAA). Cells were incubated at 37 ºC in 5%
822 CO_2 until cytopathic effects were observed at which time the supernatant was harvested and
823 filtered through a 0.2mm filter, aliquoted and stored at -80 °C.

824 **Viral suppression assay**

825 The SARS-CoV-2 viral strain, Victoria 01/20 (BVIC01), was used to infect Calu-3 cells [41,58].
826 Briefly, $1x10^5$ Calu-3 cells were seeded in flat-bottom 96-well plates 48 hours prior to infection
827 with SARS-CoV-2 at the indicated MOIs for 2h. The viral inoculum was carefully removed
828 and subsequently washed with advanced DMEM supplemented with 10% FBS, 1% GlutaMAX,

1% Sodium Pyruvate and 1% PS. CD8+ T cells were then added at E:T of 1:1, 3:1 or 4:1. Upon 15 hours post-infection (hpi), Calu-3 cells were washed with PBS thoroughly to remove CD8+ T cells. The VSA was carried out in duplicates for each condition. For q-PCR based viral suppression assay, RNA lysates of infected Calu-3 cells from each condition were then pooled for RNA extraction using a RNeasy Plus Mini Kit (Qiagen). Total RNA was then subject to one-step RT-qPCR to measure cellular viral transcription using the StepOne Real-Time PCR System (Applied Biosystem). Takyon One-Step RT Probe Mastermix (Eurogentec) and primers/probes from SARS-CoV-2 CDC EUA Kit (IDT) were used under the following PCR conditions: 50°C for 30 min, 95°C for 2 min, then anneal and extension of 95°C for 5 sec and 60°C for 30 secs running in total of 45 cycles. β2M gene (Thermofisher) was detected as the endogenous control. SARS-CoV-2 infected Calu-3 cells cultured alone or cocultured with irrelevant CD8+ T cell clones were used as controls.

For flowcytometry based viral suppression assay, Calu-3 cells post effector and target coculture were washed with PBS, trypsinized and rested in PBS on ice for 30 mins followed by viability LIVE/DEAD Fixable Aqua Dead Cell staining. Infected cells were detected by intracellular staining of anti-SARS-CoV-2-spike antibody (R&D). Cells were acquired on a LSRFortessa (BD Biosciences) and analyzed using FlowJo v10.4 (Tree Star). % Reduction of SARS-CoV2-infected Calu-3 cells was calculated by normalizing to data obtained with no effectors using the following formula: (1-fraction of spike+ cells in infected Calu-3 co-cultured with CD8+ clone cells/ fraction of spike+ cells in infected Calu-3 cultured alone) x 100

Detection of HLA-E and HLA-I expression after SARS-CoV-2 infection

Calu-3 or A549 cells overexpressing human ACE2 were tested for HLA expression after SARS-CoV-2 infection. In brief, cells were first seeded 48 hours before SARS-CoV-2 infection

at the indicated MOIs (0.01, 0.1 and 1) for 2 hours. Unbound virus was removed by washing and cells were incubated with fresh culture media supplemented with or without Remdesivir (10μM). At indicated time points (6h, 12h, 24h and 48h), cells were washed with PBS, trypsinized and maintained on ice for 30 min. The viability of Calu-3 cells was confirmed to be >99% using LIVE/DEAD Fixable Aqua Dead Cell Stain Kit. Surface or ICS staining was performed to detect surface or total HLA-E or HLA-I expression using anti-human HLA-E antibody (3D12, Biolegend) and anti-human HLA-I antibody (W6/32, Biolegend). Infected cells were detected by anti-SARS-CoV-2-spike antibody (R&D). Cells were acquired on a LSRFortessa (BD Biosciences) and analyzed using FlowJo v10.4 (Tree Star).

Primary reconstituted human airway epithelia cells MuciAir^{TM} (Epithelix, Switzerland) were reconstituted using airway epithelia cells from 14 donors. They were infected with the mNEONGreen reporter SARS-CoV-2 viral strain, pSC2-Rep-Wu-p-RL-6NG (ORF6 mNeonGreen) at M.O.I of 0.1. Successful infection was identified by green fluorescent epithelia cells. HLA-E and HLA-I expression were evaluated at 48 hours post-infection (hpi) described as above by surface staining with anti-HLA-class I antibody W6/32 and anti-HLA-E antibody 3D12.

Cloning of single chain NKG2x-CD94 soluble ectodomains

A NKG2x-CD94 ectodomain interspersed with a flexible (GGS)2 linker was cloned by splicing overlap extension PCR (Q5 Hot Start polymerase, NEB). Primers AgeI-5' NKG2x: CATGACCGGTACACAGAAAGCGCGTCATTG and 3' NKG2x GGS2: GCTACCGCCGCTACCGCCAAGCTTATGCTTACAATGATA were used to generate the NKG2x-GGS portion, and 5' GGS2 CD94: GGCGGTAGCGGCGGTAGCATTGAGCCTGCCTTTACAC plus 3' CD94-KpnI:

879 AGTCGGTACCTATCAGCTGCTGTTTGCAGATGTATCTG produced the GGS-CD94
880 portion. A second PCR step was performed on the combined initial PCR products using the
881 external AgeI-5' NKG2x - 3' CD94-KpnI primers. Following subcloning into a pCR-Blunt-II-
882 TOPO shuttle vector (Invitrogen), the product was digested (AgeI and KpnI) and cloned into
883 the pHLSec-Avitag3 expression vector [50]. DH5α *E.coli* were used for plasmid propagation and
884 sequence analysis (QIAgen miniprep and maxiprep kits).
885
886 **Expression and Purification of NKG2x-CD94 fusion proteins**
887 Biotinylated NKG2x-CD94 fusion protein was expressed using the Expi293 system
888 (ThermoFisher Scientific). Biotinylation was achieved by co-transfection with a BirA enzyme-
889 encoding pHL-BirA-KDEL vector (10:1 NKG2x: BirA vector ratios), in media supplemented
890 with 2 mM D-biotin. At 96 hours post-transfection, supernatants were clarified (by
891 centrifugation and 0.45µM PES membrane filtration), adjusted to IMAC binding conditions
892 (20mM NaPi pH8.0, 0.5M NaCl, 20mM Imidazole) and loaded onto a HisTrap FF 5ml Ni-
893 NTA column on an AKTA Pure FPLC system (Cytiva). Protein was eluted with 5CV Elution
894 buffer (20mM NaPi pH8.0, 0.5M NaCl, 300mM Imidazole), and fractions were pooled,
895 concentrated and subsequently loaded onto a Superdex 200 Increase 10/300 GL
896 chromatography column equilibrated with 20mM Tris-HCl pH8.0 150mM NaCl. Size-
897 fractionated samples were analysed by SDS-PAGE, and biotinylation was assessed using a
898 streptavidin shift assay.
899
900 **NKG2x-CD94 Tetramer staining and flow cytometry**
901 Streptavidin-APC tetramerised NKG2x-CD94 material was used to stain Δβ2m 293T cells
902 expressing single chain trimer constructs encoding peptide, β2m and HLA-E heavy chain fused
903 to EGFP. Cells were grown to approximately 60-70% confluency prior to transient

transfection using Genejuice reagent (Merck Millipore). Following EGFP expression validation at 24h post-transfection, cells were harvested, washed in ice-cold PBS and co-stained with 100ng of tetramerised NKG2x-CD94 plus 1µl of anti-β_2m mAb 2M2-PEcy7 (BioLegend), in a final volume of 100µl of PBS, for 20 minutes at 4°C. Cells were then washed and resuspended in PBS for flow cytometry using a CyAn ADP flow cytometer (Beckman Coulter). Analysis was conducted using FlowJo 10 software (Becton Dickinson).

TCR transduction into primary CD8+ T cells

Primary CD8+ TCR transductants were generated as previously described (ref H Yang Sci Imm paper). Briefly, TCR alpha and beta VDJ regions were amplified and assembled into a pHR-SIN backbone with the murine TCR alpha and beta constant regions using the HiFi DNA Assembly cloning kit (NEB). Lentiviruses were generated by transfecting the TCR-containing plasmid together with packaging plasmids pMDG-VSVG and pCMV-dR8.91 into HEK 293T cells by TurboFectin (Origene). CD8+ T cells were isolated from cone PBMC and activated with 1:1 of CD3/CD28 Dynabeads (Thermo Fisher) for 2 days, then transduced with lentiviruses. Mouse TCRβ+CD8+cells were sorted (BD Fusion) and expanded for a further 17 days before subsequent functional analysis of TCR transductants. Anti-SARS-CoV2 function of TCR transductants were assessed as described in flow based Viral Suppression Assay.

Statistical analysis

Data analysis was performed, and graphs were generated using GraphPad Prism v8. Mann Whitney test was adopted to compare difference between 2 groups where applicable.

References and Notes:

1. Strong RK, Holmes MA, Li P, Braun L, Lee N, Geraghty DE. HLA-E allelic variants. Correlating differential expression, peptide affinities, crystal structures, and thermal stabilities. *J Biol Chem.* 2003;278(7):5082-5090.
2. Apps R, Meng Z, Del Prete GQ, Lifson JD, Zhou M, Carrington M. Relative expression levels of the HLA class-I proteins in normal and HIV-infected cells. *J Immunol.* 2015;194(8):3594-3600.
3. Braud VM, Allan DS, Wilson D, McMichael AJ. TAP- and tapasin-dependent HLA-E surface expression correlates with the binding of an MHC class I leader peptide. *Curr Biol.* 1998;8(1):1-10.
4. Camilli G, Cassotta A, Battella S, et al. Regulation and trafficking of the HLA-E molecules during monocyte-macrophage differentiation. *J Leukoc Biol.* 2016;99(1):121-130.
5. Braud VM, Allan DS, O'Callaghan CA, et al. HLA-E binds to natural killer cell receptors CD94/NKG2A, B and C. *Nature.* 1998;391(6669):795-799.
6. Miller JD, Weber DA, Ibegbu C, Pohl J, Altman JD, Jensen PE. Analysis of HLA-E peptide-binding specificity and contact residues in bound peptide required for recognition by CD94/NKG2. *J Immunol.* 2003;171(3):1369-1375.
7. Hansen SG, Wu HL, Burwitz BJ, et al. Broadly targeted CD8(+) T cell responses restricted by major histocompatibility complex E. *Science.* 2016;351(6274):714-720.
8. Heinzel AS, Grotzke JE, Lines RA, et al. HLA-E-dependent presentation of Mtb-derived antigen to human CD8+ T cells. *J Exp Med.* 2002;196(11):1473-1481.
9. Joosten SA, van Meijgaarden KE, van Weeren PC, et al. Mycobacterium tuberculosis peptides presented by HLA-E molecules are targets for human CD8 T-cells with cytotoxic as well as regulatory activity. *PLoS Pathog.* 2010;6(2):e1000782.
10. Romagnani C, Pietra G, Falco M, Mazzarino P, Moretta L, Mingari MC. HLA-E-restricted recognition of human cytomegalovirus by a subset of cytolytic T lymphocytes. *Hum Immunol.* 2004;65(5):437-445.
11. Walters LC, Harlos K, Brackenridge S, et al. Pathogen-derived HLA-E bound epitopes reveal broad primary anchor pocket tolerability and conformationally malleable peptide binding. *Nat Commun.* 2018;9(1):3137.
12. Walters LC, McMichael AJ, Gillespie GM. Detailed and atypical HLA-E peptide binding motifs revealed by a novel peptide exchange binding assay. *Eur J Immunol.* 2020.
13. Malouli D, Hansen SG, Hancock MH, et al. Cytomegaloviral determinants of CD8(+) T cell programming and RhCMV/SIV vaccine efficacy. *Sci Immunol.* 2021;6(57).
14. Verweij MC, Hansen SG, Iyer R, et al. Modulation of MHC-E transport by viral decoy ligands is required for RhCMV/SIV vaccine efficacy. *Science.* 2021;372(6541).
15. Grotzke JE, Harriff MJ, Siler AC, et al. The Mycobacterium tuberculosis phagosome is a HLA-I processing competent organelle. *PLoS Pathog.* 2009;5(4):e1000374.
16. Jurtz V, Paul S, Andreatta M, Marcatili P, Peters B, Nielsen M. NetMHCpan-4.0: Improved Peptide-MHC Class I Interaction Predictions Integrating Eluted Ligand and Peptide Binding Affinity Data. *J Immunol.* 2017;199(9):3360-3368.
17. Hammer Q, Dunst J, Christ W, et al. SARS-CoV-2 Nsp13 encodes for an HLA-E-stabilizing peptide that abrogates inhibition of NKG2A-expressing NK cells. *Cell Rep.* 2022;38(10):110503.

18. Walters LC, Rozbesky D, Harlos K, et al. Primary and secondary functions of HLA-E are determined by stability and conformation of the peptide-bound complexes. *Cell Rep.* 2022;39(11):110959.
19. Toebes M, Rodenko B, Ovaa H, Schumacher TN. Generation of peptide MHC class I monomers and multimers through ligand exchange. *Curr Protoc Immunol.* 2009;Chapter 18:Unit 18 16.
20. Lampen MH, Hassan C, Sluijter M, et al. Alternative peptide repertoire of HLA-E reveals a binding motif that is strikingly similar to HLA-A2. *Mol Immunol.* 2013;53(1-2):126-131.
21. Sekine T, Perez-Potti A, Rivera-Ballesteros O, et al. Robust T Cell Immunity in Convalescent Individuals with Asymptomatic or Mild COVID-19. *Cell.* 2020;183(1):158-168 e114.
22. Rha MS, Jeong HW, Ko JH, et al. PD-1-Expressing SARS-CoV-2-Specific CD8(+) T Cells Are Not Exhausted, but Functional in Patients with COVID-19. *Immunity.* 2021;54(1):44-52 e43.
23. Peng Y, Mentzer AJ, Liu G, et al. Broad and strong memory CD4(+) and CD8(+) T cells induced by SARS-CoV-2 in UK convalescent individuals following COVID-19. *Nat Immunol.* 2020;21(11):1336-1345.
24. Nguyen THO, Rowntree LC, Petersen J, et al. CD8(+) T cells specific for an immunodominant SARS-CoV-2 nucleocapsid epitope display high naive precursor frequency and TCR promiscuity. *Immunity.* 2021;54(5):1066-1082 e1065.
25. Kared H, Redd AD, Bloch EM, et al. SARS-CoV-2-specific CD8+ T cell responses in convalescent COVID-19 individuals. *J Clin Invest.* 2021;131(5).
26. Ferretti AP, Kula T, Wang Y, et al. Unbiased Screens Show CD8(+) T Cells of COVID-19 Patients Recognize Shared Epitopes in SARS-CoV-2 that Largely Reside outside the Spike Protein. *Immunity.* 2020;53(5):1095-1107 e1093.
27. Fajnzylber J, Regan J, Coxen K, et al. SARS-CoV-2 viral load is associated with increased disease severity and mortality. *Nat Commun.* 2020;11(1):5493.
28. Zheng S, Fan J, Yu F, et al. Viral load dynamics and disease severity in patients infected with SARS-CoV-2 in Zhejiang province, China, January-March 2020: retrospective cohort study. *BMJ.* 2020;369:m1443.
29. Picelli S, Faridani OR, Bjorklund AK, Winberg G, Sagasser S, Sandberg R. Full-length RNA-seq from single cells using Smart-seq2. *Nat Protoc.* 2014;9(1):171-181.
30. Zhao Y, Zheng Z, Robbins PF, Khong HT, Rosenberg SA, Morgan RA. Primary human lymphocytes transduced with NY-ESO-1 antigen-specific TCR genes recognize and kill diverse human tumor cell lines. *J Immunol.* 2005;174(7):4415-4423.
31. Yang H, Rei M, Brackenridge S, et al. HLA-E-restricted, Gag-specific CD8(+) T cells can suppress HIV-1 infection, offering vaccine opportunities. *Sci Immunol.* 2021;6(57).
32. Huang J, Zeng X, Sigal N, et al. Detection, phenotyping, and quantification of antigen-specific T cells using a peptide-MHC dodecamer. *Proc Natl Acad Sci U S A.* 2016;113(13):E1890-1897.
33. Dolton G, Zervoudi E, Rius C, et al. Optimized Peptide-MHC Multimer Protocols for Detection and Isolation of Autoimmune T-Cells. *Front Immunol.* 2018;9:1378.
34. Davis MM, Boniface JJ, Reich Z, et al. Ligand recognition by alpha beta T cell receptors. *Annu Rev Immunol.* 1998;16:523-544.
35. Corr M, Slanetz AE, Boyd LF, et al. T cell receptor-MHC class I peptide interactions: affinity, kinetics, and specificity. *Science.* 1994;265(5174):946-949.

36. Matsui K, Boniface JJ, Steffner P, Reay PA, Davis MM. Kinetics of T-cell receptor binding to peptide/I-Ek complexes: correlation of the dissociation rate with T-cell responsiveness. *Proc Natl Acad Sci U S A.* 1994;91(26):12862-12866.
37. Einav T, Yazdi S, Coey A, Bjorkman PJ, Phillips R. Harnessing Avidity: Quantifying the Entropic and Energetic Effects of Linker Length and Rigidity for Multivalent Binding of Antibodies to HIV-1. *Cell Syst.* 2019;9(5):466-474 e467.
38. Denkberg G, Cohen CJ, Reiter Y. Critical role for CD8 in binding of MHC tetramers to TCR: CD8 antibodies block specific binding of human tumor-specific MHC-peptide tetramers to TCR. *J Immunol.* 2001;167(1):270-276.
39. Thorne LG, Reuschl AK, Zuliani-Alvarez L, et al. SARS-CoV-2 sensing by RIG-I and MDA5 links epithelial infection to macrophage inflammation. *EMBO J.* 2021:e107826.
40. Hoffmann M, Kleine-Weber H, Schroeder S, et al. SARS-CoV-2 Cell Entry Depends on ACE2 and TMPRSS2 and Is Blocked by a Clinically Proven Protease Inhibitor. *Cell.* 2020;181(2):271-280 e278.
41. Wing PAC, Keeley TP, Zhuang X, et al. Hypoxic and pharmacological activation of HIF inhibits SARS-CoV-2 infection of lung epithelial cells. *Cell Rep.* 2021;35(3):109020.
42. Zhang Y, Chen Y, Li Y, et al. The ORF8 protein of SARS-CoV-2 mediates immune evasion through down-regulating MHC-Iota. *Proc Natl Acad Sci U S A.* 2021;118(23).
43. Li Y, Renner DM, Comar CE, et al. SARS-CoV-2 induces double-stranded RNA-mediated innate immune responses in respiratory epithelial-derived cells and cardiomyocytes. *Proc Natl Acad Sci U S A.* 2021;118(16).
44. Erdmann M, Williamson MK, Jearanaiwitayakul T, Bazire J, Matthews DA, Davidson AD. Development of SARS-CoV-2 replicons for the ancestral virus and variant of concern Delta for antiviral screening. *BioRxiv.* 2022.
45. Peng Y, Felce SL, Dong D, et al. An immunodominant NP(105-113)-B*07:02 cytotoxic T cell response controls viral replication and is associated with less severe COVID-19 disease. *Nat Immunol.* 2022;23(1):50-61.
46. Keeton R, Tincho MB, Ngomti A, et al. T cell responses to SARS-CoV-2 spike cross-recognize Omicron. *Nature.* 2022;603(7901):488-492.
47. Scurr MJ, Lippiatt G, Capitani L, et al. Magnitude of venous or capillary blood-derived SARS-CoV-2-specific T cell response determines COVID-19 immunity. *Nat Commun.* 2022;13(1):5422.
48. Gao Y, Cai C, Grifoni A, et al. Ancestral SARS-CoV-2-specific T cells cross-recognize the Omicron variant. *Nat Med.* 2022;28(3):472-476.
49. Le Bert N, Tan AT, Kunasegaran K, et al. SARS-CoV-2-specific T cell immunity in cases of COVID-19 and SARS, and uninfected controls. *Nature.* 2020;584(7821):457-462.
50. Grifoni A, Weiskopf D, Ramirez SI, et al. Targets of T Cell Responses to SARS-CoV-2 Coronavirus in Humans with COVID-19 Disease and Unexposed Individuals. *Cell.* 2020;181(7):1489-1501 e1415.
51. Mallajosyula V, Ganjavi C, Chakraborty S, et al. CD8(+) T cells specific for conserved coronavirus epitopes correlate with milder disease in COVID-19 patients. *Sci Immunol.* 2021;6(61).
52. Yoo JS, Sasaki M, Cho SX, et al. SARS-CoV-2 inhibits induction of the MHC class I pathway by targeting the STAT1-IRF1-NLRC5 axis. *Nat Commun.* 2021;12(1):6602.

53. Hsu JC, Laurent-Rolle M, Pawlak JB, Wilen CB, Cresswell P. Translational shutdown and evasion of the innate immune response by SARS-CoV-2 NSP14 protein. *Proc Natl Acad Sci U S A.* 2021;118(24).
54. Coupel S, Moreau A, Hamidou M, Horejsi V, Soulillou JP, Charreau B. Expression and release of soluble HLA-E is an immunoregulatory feature of endothelial cell activation. *Blood.* 2007;109(7):2806-2814.
55. Munnur D, Teo Q, Eggermont D, et al. Altered ISGylation drives aberrant macrophage-dependent immune responses during SARS-CoV-2 infection. *Nat Immunol.* 2021;22(11):1416-1427.
56. Anjanappa R, Garcia-Alai M, Kopicki JD, et al. Structures of peptide-free and partially loaded MHC class I molecules reveal mechanisms of peptide selection. *Nat Commun.* 2020;11(1):1314.
57. Bolotin DA, Poslavsky S, Mitrophanov I, et al. MiXCR: software for comprehensive adaptive immunity profiling. *Nat Methods.* 2015;12(5):380-381.
58. Caly L, Druce J, Roberts J, et al. Isolation and rapid sharing of the 2019 novel coronavirus (SARS-CoV-2) from the first patient diagnosed with COVID-19 in Australia. *Med J Aust.* 2020;212(10):459-462.

Acknowledgements: We thank the patients and their loved ones who volunteered to contribute to this study at one of the most difficult times in their lives, and the research staff at each hospital who recruited patients at personal risk during the most extreme conditions ever witnessed in UK hospitals. This work also uses data provided by patients and collected by the NHS as part of their care and support #DataSavesLives. We are grateful to Claudia Rubio for excellent technical assistance and William James (Sir William Dunn School of Pathology, University of Oxford) for generous provision of SARS-CoV-2 strains. Calu-3 cells were kindly provided by Anderson Ryan (Oncology Department, University of Oxford). A549-ACE2 cells were kindly provided by Alfredo Castello (CVR, University of Glasgow). The pHLSec-Avitag3 vector was a kind gift from Prof. Radu Aricescu (MRC LMB, Cambridge).

Funding: This work was supported by grants from the Bill and Melinda Gates Foundation (BMGF OPP1133649), the Chinese Academy of Medical Sciences (CAMS) Innovation Fund for Medical Sciences (CIFMS 2018-I2M-2-002), the UK Medical Research Council (MRC) funded Human Immunology Unit, MRC project grant MR/R022011/1, the Oxfordshire Health Services Research Committee reference 1308, NIHR Biomedical Research Centre, Oxford, Department of Health and Social Care UKRI/NIHR COVID-19 Rapid Response Grant (COVI9-RECPLA) and Wellcome Trust grant 109965MA.

HBY and SB received support from the Chinese Academy of Medical Sciences (CAMS) Innovation Fund for Medical Science (CIFMS), China (grant number: 2018-I2M-2-002). HS is supported by CIFMS 2018-I2M-2-002 and the China Scholarship Council. JMcK is supported by a Wellcome Trust Investigator Award (IA) 200838/Z/16/Z, LT holds a Wellcome Trust fellowship [205228/Z/16/Z] and is also supported by the National Institute for Health Research Health Protection Research Unit (HPRU) in Emerging and Zoonotic Infections (NIHR200907) at University of Liverpool in partnership with Public Health England (PHE),

in collaboration with Liverpool School of Tropical Medicine and the University of Oxford. AJM is an NIHR Academic Clinical Lecturer, and AJM and PB are Jenner Institute Investigators. P.J.M.O. is supported by a NIHR Senior Investigator Award (award 201385). ISARIC4C is supported by grants from the Medical Research Council (grant MC_PC_19059), the National Institute for Health Research (NIHR) (award CO-CIN-01) and by the NIHR Health Protection Research Unit (HPRU) in Emerging and Zoonotic Infections at University of Liverpool in partnership with Public Health England (PHE), in collaboration with Liverpool School of Tropical Medicine and the University of Oxford (award 200907), NIHR HPRU in Respiratory Infections at Imperial College London with PHE (award 200927), Welcome Trust and Department for International Development (215091/Z/18/Z), and the Bill and Melinda Gates Foundation (OPP1209135), the Liverpool Experimental Cancer Medicine Centre (grant reference: C18616/A25153), NIHR Biomedical Research Centre at Imperial College London (IS-BRC-1215-20013), and the NIHR Clinical Research Network provided infrastructure support for this research.

Author contributions:

HBY, HS, GMG, JMcK and AJMcM designed and performed the experiments, analyzed the data, and wrote the manuscript.

PB and PK critically reviewed the manuscript and analyzed data.

SB, LW, GMG predicted and tested HLA-E binding peptides.

SB and LG conducted the SCT assays.

MQ performed DSF assays and generated HLA-E proteins.

XDZ, PACW conducted SARS-CoV-2 viral infection in the CL3 laboratory.

XY, SLF, YCP, TD contributed to TCR sequencing and analysis.

BW, YCP, TD generated A*24 CD8+ T cell clone

MR, JDCG, AT, BP made TCR transductants.

SM, MGS, LCQT, PJMO, JKB, AJM, PK and ISARIC4C provided samples from COVID-19 patients.

All authors read and approved the manuscript.

Competing interests: The authors declare no competing interests.

Data and materials availability: All data are available in the main text or the supplementary materials.

Table 1. TCR usage of HLA-E restricted SARS-CoV-2 specific CD8+ T cell clones

Clone	Epitope	CDR3_alpha	TRAV	TRAJ	TCRα reads *	CDR3_beta	TRBV	TRBJ	TCRβ reads *
1106 C01	P001	CAVSDTGNQFYF	TRAV21	TRAJ49	99%	CASSLFGGAHGYTF	TRBV11-2	TRBJ1-2	98%
1106 C05	P001	CALGEGYTGANSKLTF	TRDV1	TRAJ56	100%	CAWSVVGQGAPRYGYTF	TRBV30	TRBJ1-2	99%
1504 C43	P001	CAVGASDGQKLLF	TRAV21	TRAJ16	95%	CASRPRGSGTGELFF	TRBV7-9	TRBJ2-2	94%
1106 C04	P006	CVVNPLTNFGNEKLTF	TRAV12-1	TRAJ48	94%	CASSTEVSTNEKLFF	TRBV27	TRBJ1-4	98%
1106 C37	P006	CAVRSSGGSYIPTF	TRAV1-2	TRAJ6	99%	CASSTGDSNQPQHF	TRBV3-1	TRBJ1-5	99%
1106 C03	P015	CVVNPNNDMRF CAMRGSDKLIF	TRAV12-1 TRAV14DV4	TRAJ43 TRAJ34	50% 50%	CASSEDSFLNTEAFF	TRBV6-1	TRBJ1-1	100%
1106 C16	P015	CAVGNQAGTALIF	TRAV8-3	TRAJ15	99%	CASSYNPSSGEAFF	TRBV6-5	TRBJ1-1	100%
1106 C32	P015	CAESTDTGRRALTF	TRAV5	TRAJ5	100%	CSVEGQGAPGYTF	TRBV29-1	TRBJ1-2	100%
1106 C08	P015	CALYTGGFKTIF	TRAV17	TRAJ9	100%	CASRSGGLDEQFF	TRBV19	TRBJ2-1	99%
1504 C03	P015	CAVPSGTYKYIF	TRAV5	TRAJ40	100%	CASRTRQPGLGNNEQFF	TRBV6-5	TRBJ2-1	100%
1504 C24	P015	CAVEEGFQKLVF CILRDWDGTASKLTF	TRAV22 TRAV26-2	TRAJ8 TRAJ44	51% 48%	CASSQDSGNEQFF	TRBV4-1	TRBJ2-1	98%
1504 C09	P015	CAESAYGGSQGNLIF	TRAV5	TRAJ42	99%	CASSAGETQYF	TRBV25-1	TRBJ2-5	99%
1106 C17	P015	CAMREERNARLMF CAVRDGGGYGGATNKLIF	TRAV14DV4 TRAV3	TRAJ31 TRAJ32	85% 14%	CASSHSTGVYEQYF	TRBV7-9	TRBJ2-7	100%

*Total reads from TCR sequencing were 81576 (median, IQR: 40624-161076).